

AD-A254 648



2

**Carderock Division
Naval Surface Warfare Center**

Bethesda, MD 20084-5000

CARDEROCKDIV/SHD-1392-01 July 1992

Ship Hydromechanics Department

Departmental Report

**Experimental Investigation of
the Effect of Above Water Bow
Shape on Flare Slamming and
Deck Wetness Forces**

by

Harry D. Jones



92 9 01 03

92-24286



424913

3798



Approved For Public Release, Distribution Unlimited. July 1992.

MAJOR DTRC TECHNICAL COMPONENTS

CODE 011 DIRECTOR OF TECHNOLOGY, PLANS AND ASSESSMENT

12 SHIP SYSTEMS INTEGRATION DEPARTMENT

14 SHIP ELECTROMAGNETIC SIGNATURES DEPARTMENT

15 SHIP HYDROMECHANICS DEPARTMENT

16 AVIATION DEPARTMENT

17 SHIP STRUCTURES AND PROTECTION DEPARTMENT

18 COMPUTATION, MATHEMATICS & LOGISTICS DEPARTMENT

19 SHIP ACOUSTICS DEPARTMENT

27 PROPULSION AND AUXILIARY SYSTEMS DEPARTMENT

28 SHIP MATERIALS ENGINEERING DEPARTMENT

DTRC ISSUES THREE TYPES OF REPORTS:

1. **DTRC reports, a formal series**, contain information of permanent technical value. They carry a consecutive numerical identification regardless of their classification or the originating department.
2. **Departmental reports, a semiformal series**, contain information of a preliminary, temporary, or proprietary nature or of limited interest or significance. They carry a departmental alphanumerical identification.
3. **Technical memoranda, an informal series**, contain technical documentation of limited use and interest. They are primarily working papers intended for internal use. They carry an identifying number which indicates their type and the numerical code of the originating department. Any distribution outside DTRC must be approved by the head of the originating department on a case-by-case basis.

UNCLASSIFIED

SECURITY CLASSIFICATION OF THIS PAGE

REPORT DOCUMENTATION PAGE				Form Approved OMB No. 0704-0188	
1a. REPORT SECURITY CLASSIFICATION UNCLASSIFIED			1b. RESTRICTIVE MARKINGS		
2a. SECURITY CLASSIFICATION AUTHORITY			3. DISTRIBUTION / AVAILABILITY OF REPORT (see reverse side)		
2b. DECLASSIFICATION / DOWNGRADING SCHEDULE					
4. PERFORMING ORGANIZATION REPORT NUMBER(S) CARDEROCKDIV/SHD-1392-01			5. MONITORING ORGANIZATION REPORT NUMBER(S)		
6a. NAME OF PERFORMING ORGANIZATION Carderock Division, NSWC Ship Hydromechanics Dept.		6b. OFFICE SYMBOL (If applicable) Code 1561	7a. NAME OF MONITORING ORGANIZATION Carderock Division, Naval Surface Warfare Center		
6c. ADDRESS (City, State, and ZIP Code) Bethesda, Maryland 20084-5000			7b. ADDRESS (City, State, and ZIP Code) Bethesda, Maryland 20084-5000		
8a. NAME OF FUNDING / SPONSORING ORGANIZATION I. E. D and G. H. R.		8b. OFFICE SYMBOL (If applicable)	9. PROCUREMENT INSTRUMENT IDENTIFICATION NUMBER		
8c. ADDRESS (City, State, and ZIP Code) Department of the Navy Bethesda, Maryland 20084-5000			10. SOURCE OF FUNDING NUMBERS		
			PROGRAM ELEMENT NO	PROJECT NO.	TASK NO
11. TITLE (Include Security Classification) Experimental Investigation of the Effect of Above Water Bow Shape on Flare Slamming and Deck Wetness Forces					
12. PERSONAL AUTHOR(S) H.D. Jones					
13a. TYPE OF REPORT Final		13b. TIME COVERED FROM 800930 TO 820930		14. DATE OF REPORT (Year, Month, Day) 1992 July	
15. PAGE COUNT 32					
16. SUPPLEMENTARY NOTATION					
17. COSATI CODES			18. SUBJECT TERMS (Continue on reverse if necessary and identify by block number) Seaworthiness, Deck Wetness, Flare Slamming, Above Water Bow Shape, Model Experiments.		
FIELD	GROUP	SUB-GROUP			
19. ABSTRACT (Continue on reverse if necessary and identify by block number) The Carderock Division, Naval Surface Warfare Center undertook to experimentally determine the effects of above water bow shape on vertical flare slam and deck wetness loadings. A modern naval combatant was selected as the parent hull form and six variations in the above water bow shape were investigated. It is shown that significant variations in the flare slam forces occur with changing bow shape while deck wetness forces remain relatively constant.					
20. DISTRIBUTION / AVAILABILITY OF ABSTRACT <input type="checkbox"/> UNCLASSIFIED/UNLIMITED <input checked="" type="checkbox"/> SAME AS RPT <input type="checkbox"/> DTIC USERS			21. ABSTRACT SECURITY CLASSIFICATION UNCLASSIFIED		
22a. NAME OF RESPONSIBLE INDIVIDUAL Harry D. Jones			22b. TELEPHONE (Include Area Code) 301-227-1210		22c. OFFICE SYMBOL Code 1561

UNCLASSIFIED

SECURITY CLASSIFICATION OF THIS PAGE

(BLOCK 3)

Approved For Public Release, Distribution Unlimited. July 1992.

Accession For	
NTIS CRA&I	<input checked="checked" type="checkbox"/>
DTIC TAB	<input type="checkbox"/>
Unannounced	<input type="checkbox"/>
Justification	
By	
Distribution /	
Availability Codes	
Dist	Avail and/or Special
A-1	

DTIC QUALITY INSPECTED 3

CONTENTS

	Page
ABSTRACT	1
ADMINISTRATIVE INFORMATION	1
INTRODUCTION	1
MODEL PARTICULARS	1
INSTRUMENTATION	2
MEASUREMENT UNCERTAINTY	3
EXPERIMENTAL PROCEDURE	3
DATA ANALYSIS	3
RESULTS AND DISCUSSION	4
CONCLUSIONS	5
REFERENCES	31

FIGURES

	Page
1. Parent Hull Body Plan	6
2. Above Water Variations for Bows 1 and 2 Compared to the Parent	7
3. Above Water Variations for Bows 3 and 4 Compared to the Parent	8
4. Above Water Variations for Bows 5 and 6 Compared to the Parent	9
5. Example Time Histories Illustrating the Combination of Force Components	10
6. Nondimensional Pitch Transfer Function Comparing the Parent (P) with the Six Bow Variants (1-6)	11
7. Nondimensional Heave Transfer Function Comparing the Parent (P) with the Six Bow Variants (1-6)	12
8. Nondimensional Acceleration Transfer Function Comparing the Parent (P) with the Six Bow Variants (1-6)	13
9. Nondimensional Relative Bow Motion Transfer Function Forward of the Stem Comparing the Parent (P) with the Six Bow Variants (1-6)	14
10. Nondimensional Relative Bow Motion Transfer Function at Station 0 Port Side Comparing the Parent (P) with the Six Bow Variants (1-6)	15
11. Nondimensional Relative Bow Motion Transfer Function at Station 1 Star- board Side Comparing the Parent (P) with the Six Bow Variants (1-6)	16
12. Nondimensional Relative Bow Motion Transfer Function at Station 2 Port Side Comparing the Parent (P) with the Six Bow Variants (1-6)	17
13. Peak Flare Slam and Deck Wetness Forces Acting on the Parent Bow Normalized by Wave Amplitude	18

14. Peak Flare Slam and Deck Wetness Forces Acting on Bow 1 Normalized by Wave Amplitude	19
15. Peak Flare Slam and Deck Wetness Forces Acting on Bow 2 Normalized by Wave Amplitude	20
16. Peak Flare Slam and Deck Wetness Forces Acting on Bow 3 Normalized by Wave Amplitude	21
17. Peak Flare Slam and Deck Wetness Forces Acting on Bow 4 Normalized by Wave Amplitude	22
18. Peak Flare Slam and Deck Wetness Forces Acting on Bow 5 Normalized by Wave Amplitude	23
19. Peak Flare Slam and Deck Wetness Forces Acting on Bow 6 Normalized by Wave Amplitude	24
20. Peak Flare Slam and Deck Wetness Forces Acting on the Parent Bow versus Wave Height in Head Waves for $\lambda/L = 1.2$ and $F_n = 0.30$	25
21. Peak Flare Slam and Deck Wetness Forces Acting on Bow 1 and Bow 2 versus Wave Height in Head Waves for $\lambda/L = 1.2$ and $F_n = 0.30$	26
22. Peak Flare Slam and Deck Wetness Forces Acting on Bow 3 and Bow 4 versus Wave Height in Head Waves for $\lambda/L = 1.2$ and $F_n = 0.30$	27
23. Peak Flare Slam and Deck Wetness Forces Acting on Bow 5 and Bow 6 versus Wave Height in Head Waves for $\lambda/L = 1.2$ and $F_n = 0.30$	28

TABLES

	Page
1. Flare Slamming Model Particulars	29

ABSTRACT

The Carderock Division, Naval Surface Warfare Center undertook to experimentally determine the effects of above water bow shape on vertical flare slam and deck wetness loadings. A modern naval combatant was selected as the parent hull form and six variations in the above water bow shape were investigated. It is shown that significant variations in the flare slam forces occur with changing bow shape while deck wetness forces remain relatively constant.

ADMINISTRATIVE INFORMATION

This work was conducted at the Carderock Division, Naval Surface Warfare Center (CARDEROCKDIV, NSWC) in support of the Independent Exploratory Development Program of the CARDEROCKDIV, NSWC and the General Hydromechanics Research Program sponsored by the Naval Sea Systems Command and administered by the CARDEROCKDIV, NSWC.

INTRODUCTION

In general, Naval combatant hulls of the World War II era had relative fine bow form with little flat bottom and almost no bow flare. Bottom slam impact forces were small but deck wetness was severe. Current ship designs include substantial amounts of bow flare in an effort to increase usable deck area with a minimum of wetness. As a result, local bow flare impacts are a source of concern.

This experimental investigation was carried out during 1981 and 1982 to establish a useful data base as to the effects of above water bow shape on motions and loadings due to flare slamming impact and deck wetness.

A parent hull form was selected for this study which was representative of a modern combatant. A set of six above water bow variations were then designed to produce what was considered a range of realistic variations in bow shape. Some of the deck wetness results have been previously published¹. The present report presents the results of the experimental program.

MODEL PARTICULARS

Particulars for the model used in this investigation are given in Table 1, with the parent body plan shown in Figure 1. The six above water variations in bow shape are compared to the parent in Figures 2 through 4. The 4.5 meter model was constructed of Fiberglas at the CARDEROCKDIV, NSWC and designated Model 5405. The model was designed for use with the CARDEROCKDIV, NSWC pogo stick seakeeping towing and motion measuring device and therefore was not equipped with propulsion or rudders.

The model was constructed such that the above water portion forward of Station 10 was removable. The parent as well as the six bow shape variations were constructed for installation on the basic model. These above water portions were constructed in two sections. The portion from Station 10 to Station 2.5 was rigidly attached directly to the hull with its primary function to provide a smooth transition for each bow variant to the parent hull form. The portion from Station 2.5 forward was attached to the main hull by a system of three block gages such that any vertical forces acting upon the above water bow section could be measured. The particulars of these above water bow sections (Station 2.5 forward) are presented in Table 1.

INSTRUMENTATION

This experimental investigation into the effects of above water bow shape on flare slamming and deck wetness was carried out in the Maneuvering and Seakeeping Facility (MASK) at the CARDEROCKDIV, NSWC. Throughout the experiments the model was attached to the CARDEROCKDIV, NSWC's seakeeping model towing pogo stick. This allowed the model to be towed by the MASK carriage with freedom to move in pitch, heave and roll while being restrained in surge, sway and yaw.

The pogo stick is equipped to measure pitch, heave and roll motions by potentiometers. The vertical forces acting on the bow section were measured using variable reluctance block gages mounted in a triangular array. A vertical accelerometer (Acceleration 1) was installed within the bow section to aid in determining the inertial effects of the bow section on the measured vertical forces. A second accelerometer (Acceleration 2) was installed at Station 4 as a backup to Acceleration 1 in the bow section.

The near hull relative motion around the bow section was measured by variable resistance wire probes. These were installed around the bow sections by means of a cantilever support such that no interference would be made to the force measurements, i.e., no contact with the bow section. The arrangement allowed the range of the relative motion measurement of the wire probes to extend from a few inches below the keel to a few inches above the deck level and helped avoid dropout during bow emersion and immersion. The first of the resistance probes (WP1) was installed directly forward of the stem. They were also installed at the forward perpendicular on the port (WP2) and starboard (WP3) side, at Station 1 on the port (WP4) and starboard (WP5) side and at Station 2 on the port (WP6) and starboard (WP7) side. The water on the deck of each bow section was also measured by variable resistance wire probes. These were arranged in an array of five probes placed vertically on the bow deck section. The first of these was placed on the centerline at Station 0, the next three were at Station 1 with one on the centerline, one 3 inches to port and the other 3 inches to starboard, and the fifth one was installed on the centerline at Station 2. These probes provided the depth of the water on the deck during wetness. More detailed information including drawings showing the set up for these bow section measurements and their use in a pilot experiment to determine their feasibility has been previously presented by Bales².

MEASUREMENT UNCERTAINTY

Three individual error sources must be considered in the determination of the measurement uncertainty intervals associated with the type data presented herein. These three error sources occur in calibration, data acquisition and data reduction. These measurement errors have two parts; the fixed error or bias and the random error or precision.

During the calibration process, the bias is derived from the accuracy of the calibration standard used for reference. For the data presented here, two types of mechanical reference were utilized. The angular measurements and the accelerations were calibrated on a mechanical tilt table estimated to be accurate to within 0.050 degrees and the linear displacement measurement was calibrated on a movable staff estimated to be accurate to within 0.0254 centimeters. The precision index for the calibration was derived by linear regression of the calibration values about the calibration factor used in converting the measurement voltage to physical units.

In the data acquisition process, the primary error sources are bias and occur in the instruments themselves and the analog to digital converter (A/D) used in collecting the data. The instrument errors are those stated by the manufacturer or estimated for those made in house. The A/D is considered accurate to within 0.00488 volts, which when operated on by the calibration factor, provides its bias for each channel.

The precision of the computer used in reducing the data, provides negligible error sources in the data reduction process.

The individual bias and precision error sources can be root sum squared to provide an overall bias and precision error for each measurement. From this measurement uncertainty confidence intervals of 99% and 95% can be determined.

EXPERIMENTAL PROCEDURE

The flare slamming experimental program consisted of runs in long-crested regular waves for two headings and three Froude numbers for each of the seven bows investigated. Each of the bows was examined in head (180°) and bow (210°) regular waves at Froude numbers (F_n) of 0.15, 0.30 and 0.40. It was originally intended that a Froude number of 0.45 be run, however this proved to be unreasonable for the pogo stick towing gear and was therefore reduced to 0.40. A range of long-crested regular waves of wavelength to ship length ratios from 0.8 to 3.0 were investigated with a nominal wave steepness (h/λ) of $1/30$ for the speeds and headings indicated. Linearity studies were carried out at motion resonance for all the bows particularly at a Froude number of 0.30 in head waves.

DATA ANALYSIS

Throughout the experiments the model responses were recorded in analog form on magnetic tape as well as being digitized and recorded by the on-carriage computer.

Preliminary analysis of the data was done during the experiments to monitor the results. The responses were also monitored visually on strip chart recorders during the experiment.

The recorded impact data was analyzed after testing. The analog tapes were computer digitized at a very high sample rate (125 samples/second) generating digital tapes for analysis. The raw data was resolved into the vertical force components due to flare slamming and deck wetness. To do this the vertical forces measured by each of the force block gages were combined by summing in the time domain to produce the resultant vertical force time history. The inertial force of each bow was determined by multiplying the mass of each bow times the vertical acceleration of the bow. This inertial force was then subtracted from the total force to determine the hydrodynamic loading on the bow sections. The force due to deck wetness was determined by averaging the depth of water on the deck measured by the five deck wetness probes and multiplying by the specific weight of the water and the deck area. This deck wetness force was then subtracted from the hydrodynamic force to determine the flare slamming force. An example of the time histories as they are broken down in the above description is presented in Figure 5.

The regular wave motion results were harmonic analyzed to produce the pitch, heave, acceleration and relative motion transfer functions presented herein.

RESULTS AND DISCUSSION

The results of this above water bow shape investigation are presented in Figures 6 through 23. The nondimensional transfer functions comparing the motions of each model bow configuration investigated are presented in Figures 6 through 12 for the three Froude numbers (0.15, 0.30 and 0.40) in head and bow long-crested regular waves. The pitch, heave and acceleration results presented in Figures 6 through 8 indicate the consistency of these results throughout the program. The variation in some of the relative motion results with bow configuration as presented in Figures 9 through 12 give an indication of the effect of changes in bow shape on the near hull relative motion.

The flare slam and deck wetness force results are presented in Figures 13 through 23. The curves presented in these figures were derived by hand faring lines through the experimental data for each bow. The flare slam forces presented are those impact forces acting on the bow section in a vertically up direction while the deck wetness forces are those acting vertically downward. These impact loadings are presented in Figures 13 through 19 versus wavelength to ship length ratio for Froude numbers of 0.15, 0.30 and 0.40 at headings of 180° and 210° for the parent bow and the six bow shape variations. Here the peak forces are normalized by the wave amplitude to help eliminate inconsistencies due to small wave height variations. The scatter remaining in the results is an indication of the nonlinear nature of the forces with wave amplitude.

The major vertical loading on the bow sections is due to flare impact forces. Bow 1, the Reduced Flare bow, is the only bow in which the deck wetness force approaches

the flare impact force. The increase in flare slamming and deck wetness forces with increasing Froude number can also be seen in Figures 13 through 19 as well as a slight reduction in going from head to bow waves. Presented in Figures 20 through 23 are the flare slam and deck wetness forces versus wave height for a Froude number of 0.30 and wavelength to ship length ratio of 1.2. These results indicate that changes in bow shape thought to reduce deck wetness result in significant increases in flare slamming loads while the deck wetness loads remain relatively constant. It should be noted that changes in deck area affect the depth of water on deck necessary to maintain constant loadings for the increased and decreased flare cases, i.e., the greater deck area of the increased flare requires less depth of water on deck for a given loading than does the lesser area of the decreased flare. The effectiveness of the knuckle variants in reducing wetness in less severe conditions may be decreased as they become submerged during the more severe conditions of this investigation. Effects of bow shapes on the amount of spray over the deck in less severe conditions is not investigated here.

CONCLUSIONS

The results presented herein give a comprehensive comparison of the vertical slamming loads acting on the variations of the above water bow sections investigated. Significant differences in the flare slam loads can be seen with changes in the bow shape while the deck wetness loads seem relatively unaffected.

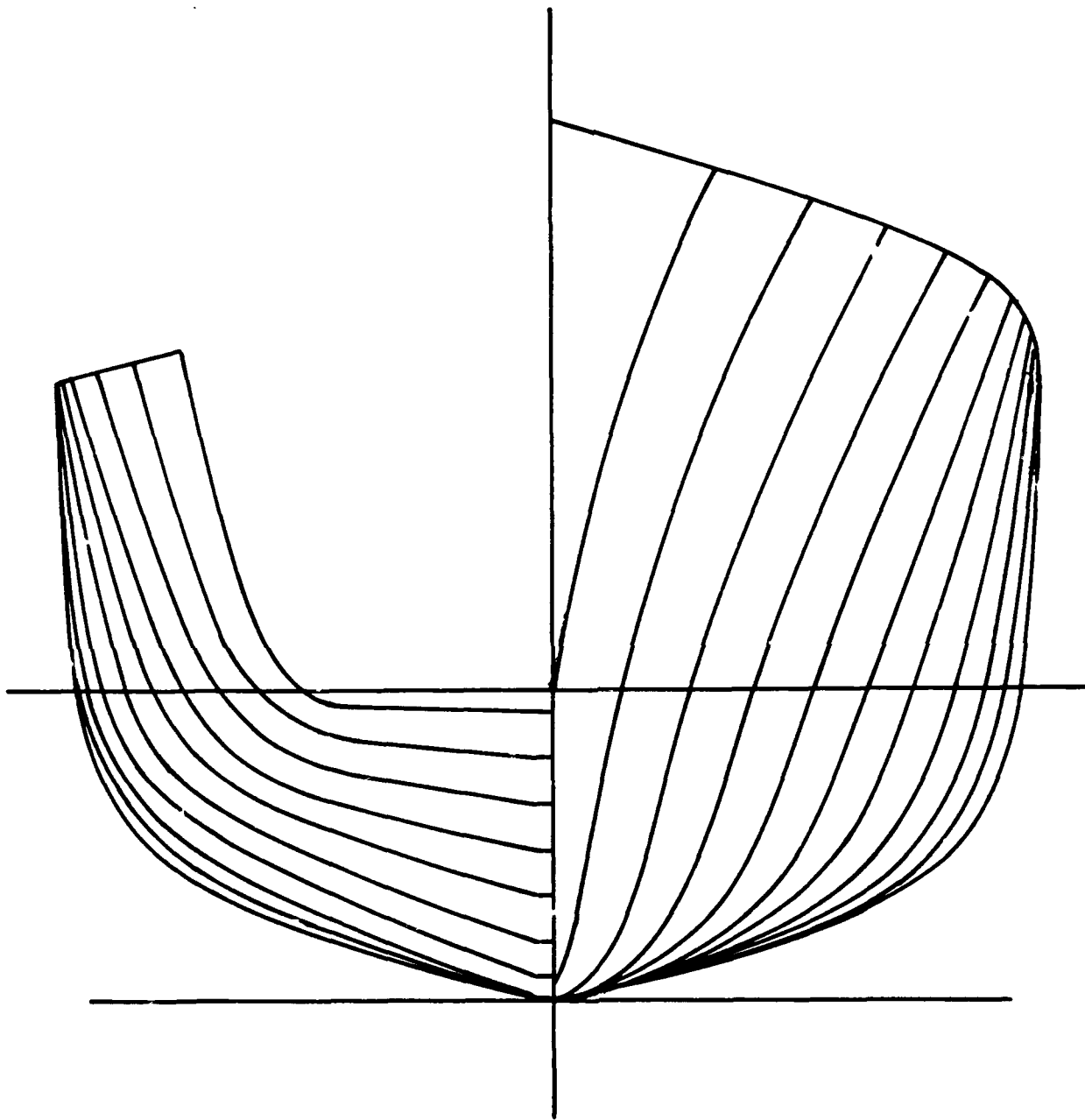
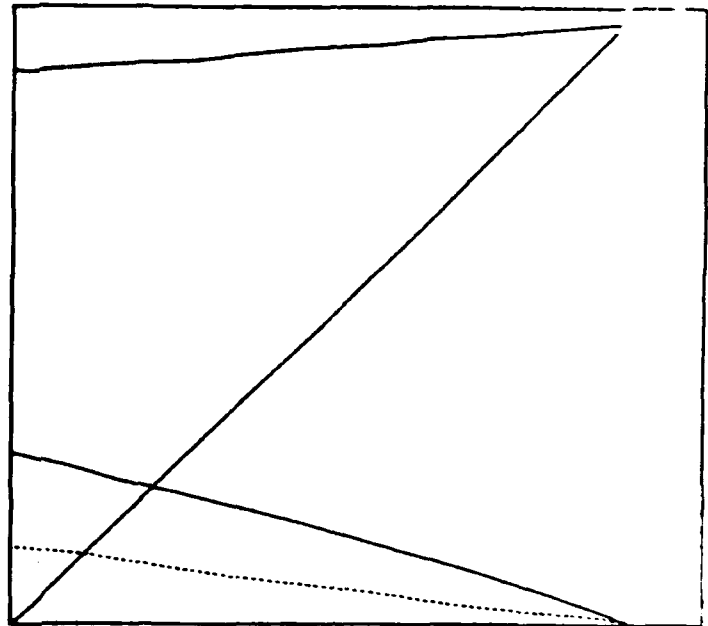
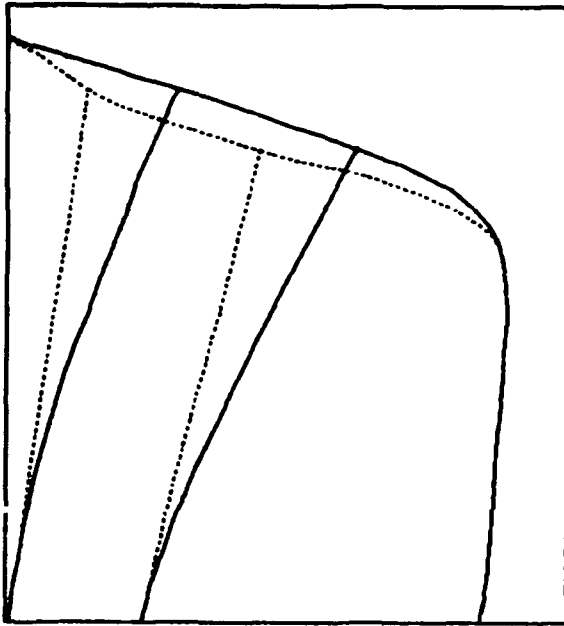
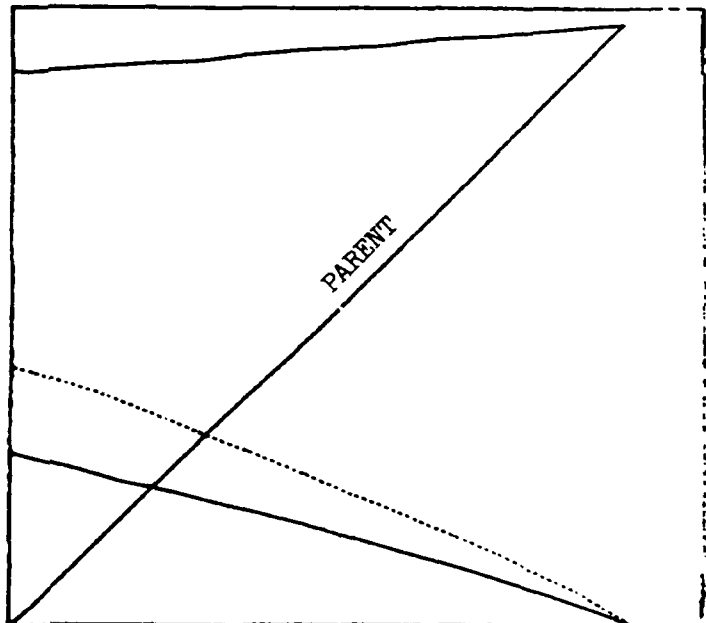
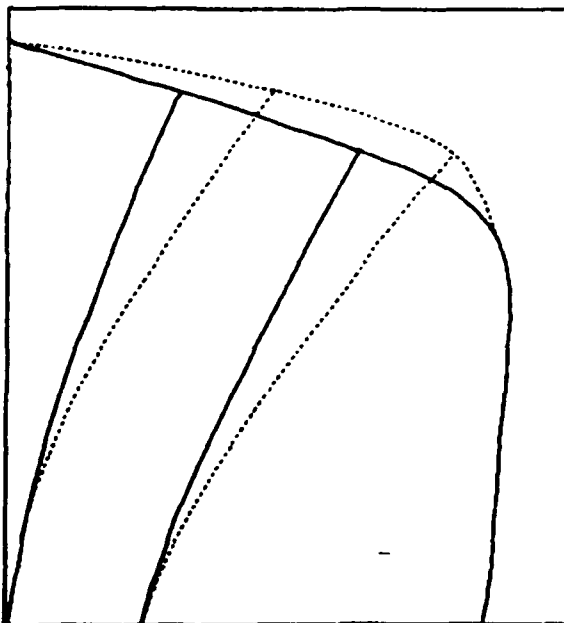


Figure 1 - Parent Full Body Plan

BOW 1
DECREASED FLARE



BOW 2
INCREASED FLARE

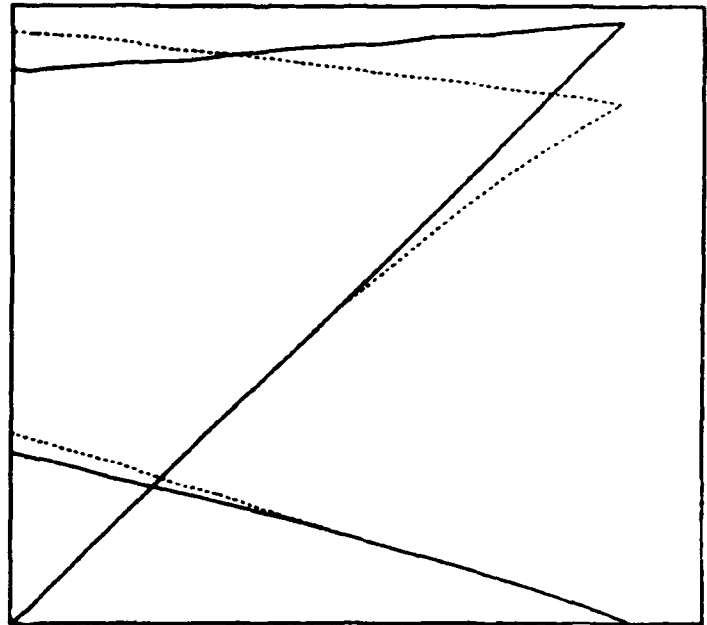
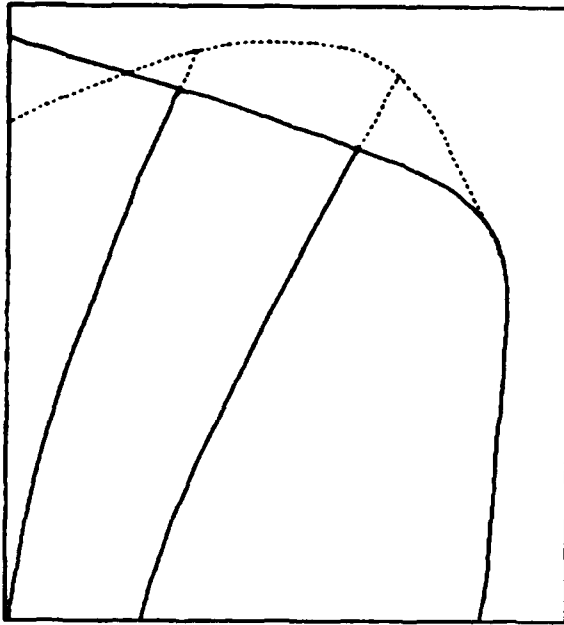


STATIONS 0, 2, AND 10

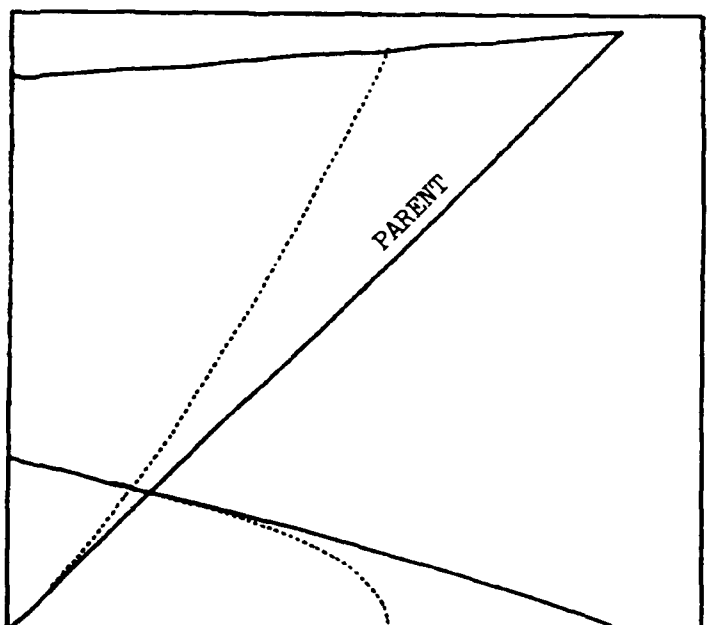
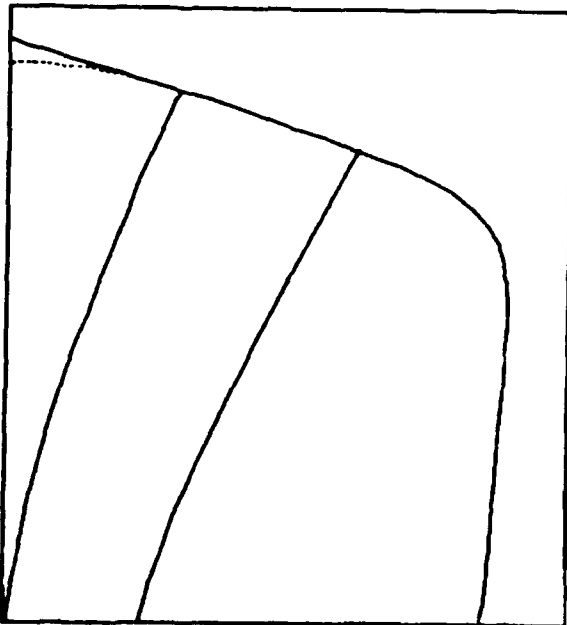
BOW PROFILE

Figure 2 - Above Water Variations for Bows 1 and 2 Compared to the Parent

BOW 3
REFLEXIVE SHEER



BOW 4
REDUCED OVERHANG

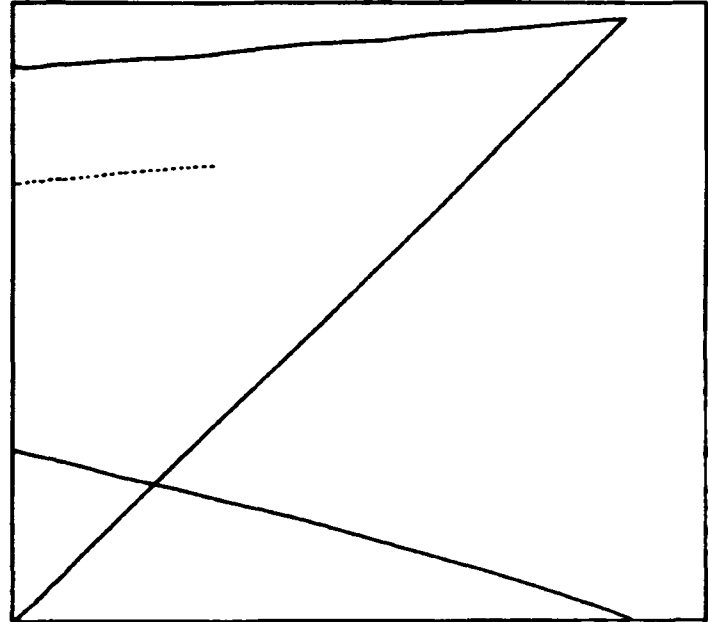
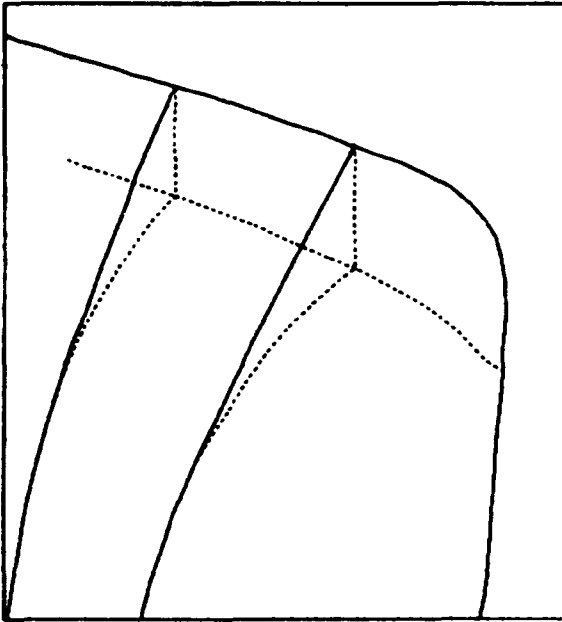


STATIONS 0, 2, AND 10

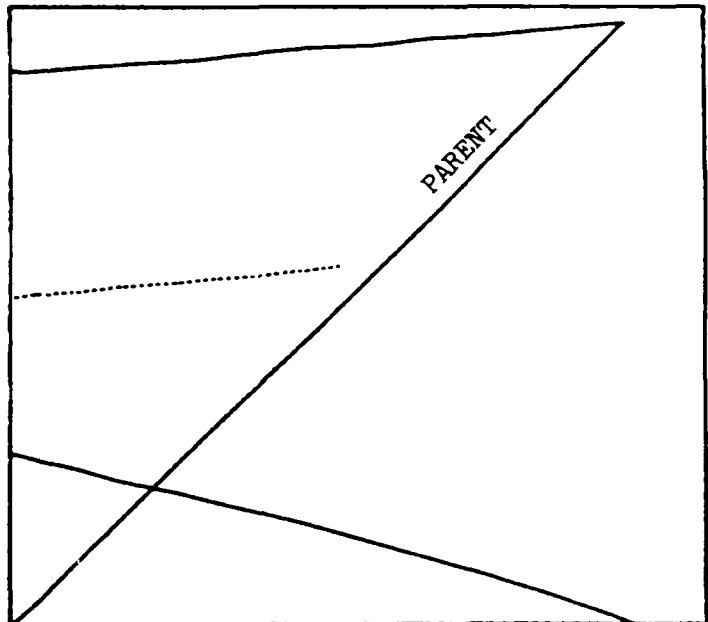
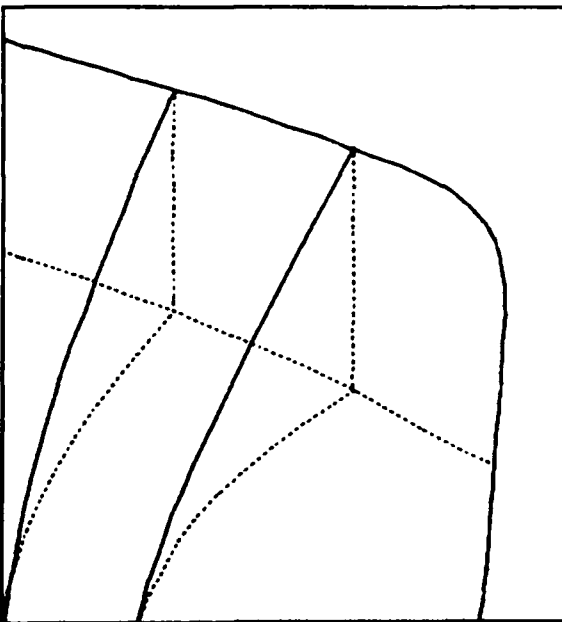
BOW PROFILE

Figure 3 - Above Water Variations for Bows 3 and 4 Compared to the Parent

BOW 5
SHALLOW KNUCKLE



BOW 6
DEEP KNUCKLE



STATIONS 0, 2, AND 10

BOW PROFILE

Figure 4 - Above Water Variations for Bows 5 and 6 Compared to the Parent

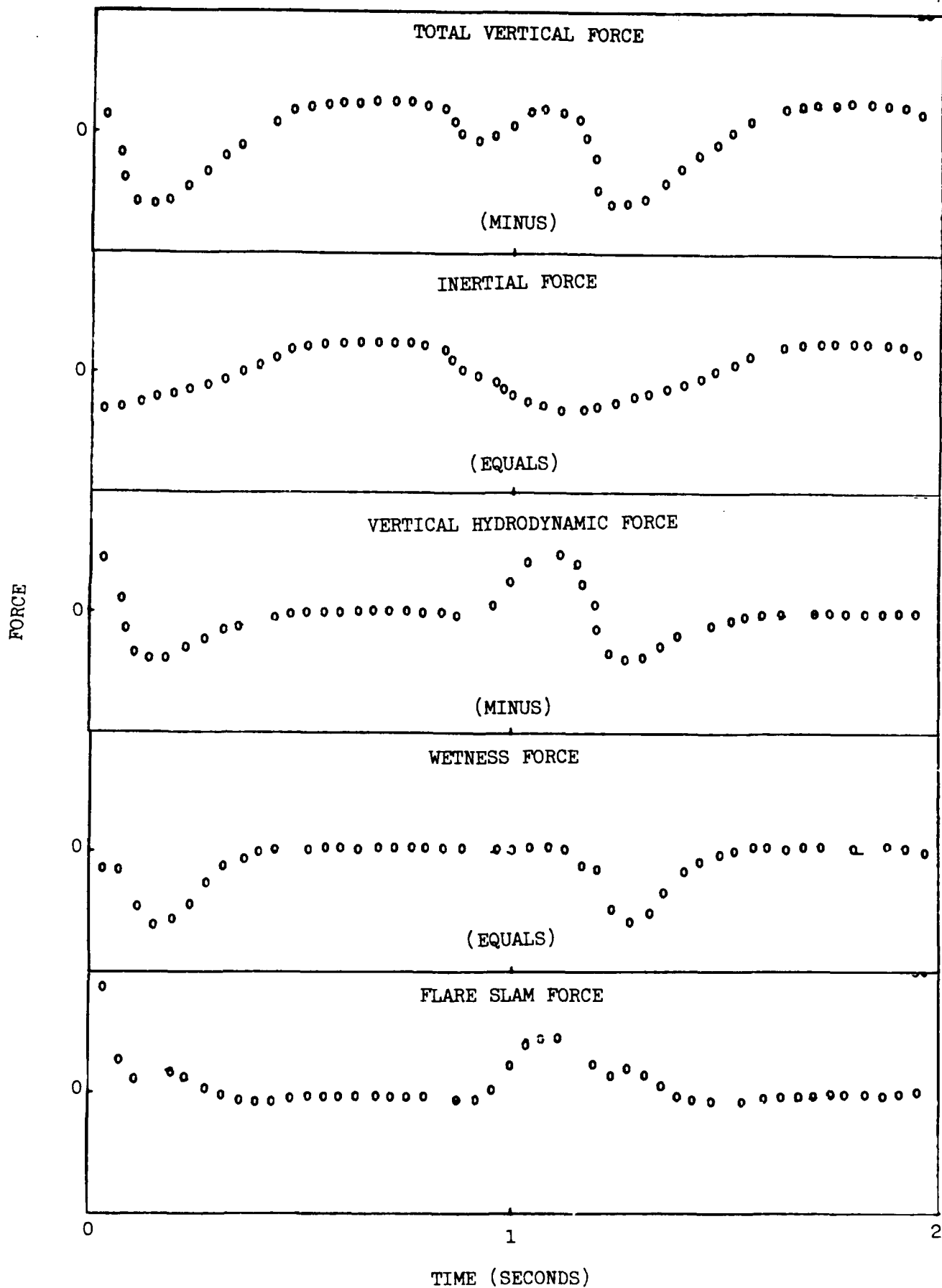


Fig. 5. Example Time Histories Illustrating the Combination of Force Components

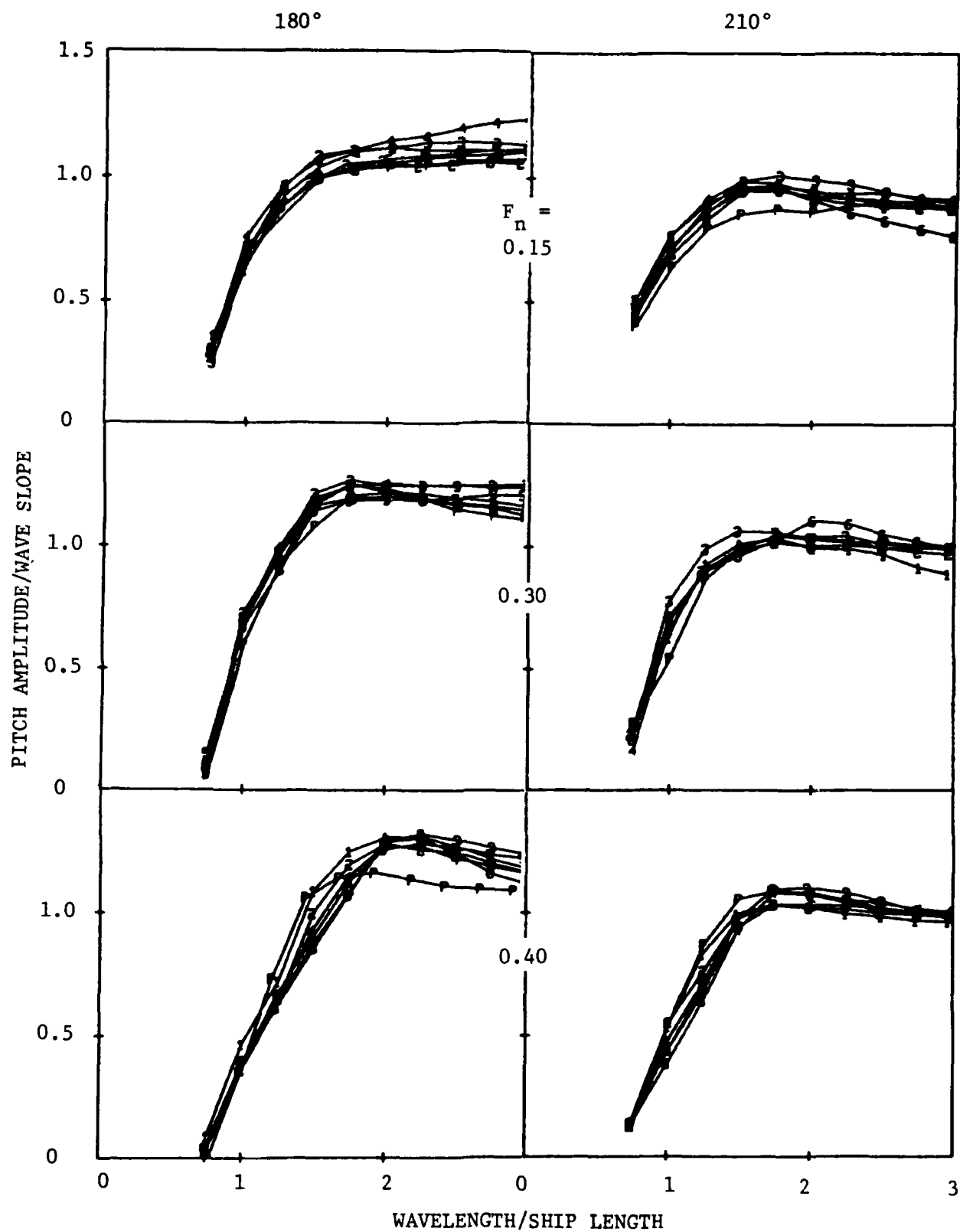


Figure 6 - Nondimensional Pitch Transfer Function Comparing the Parent (P) with the Six Bow Variants (1-6)

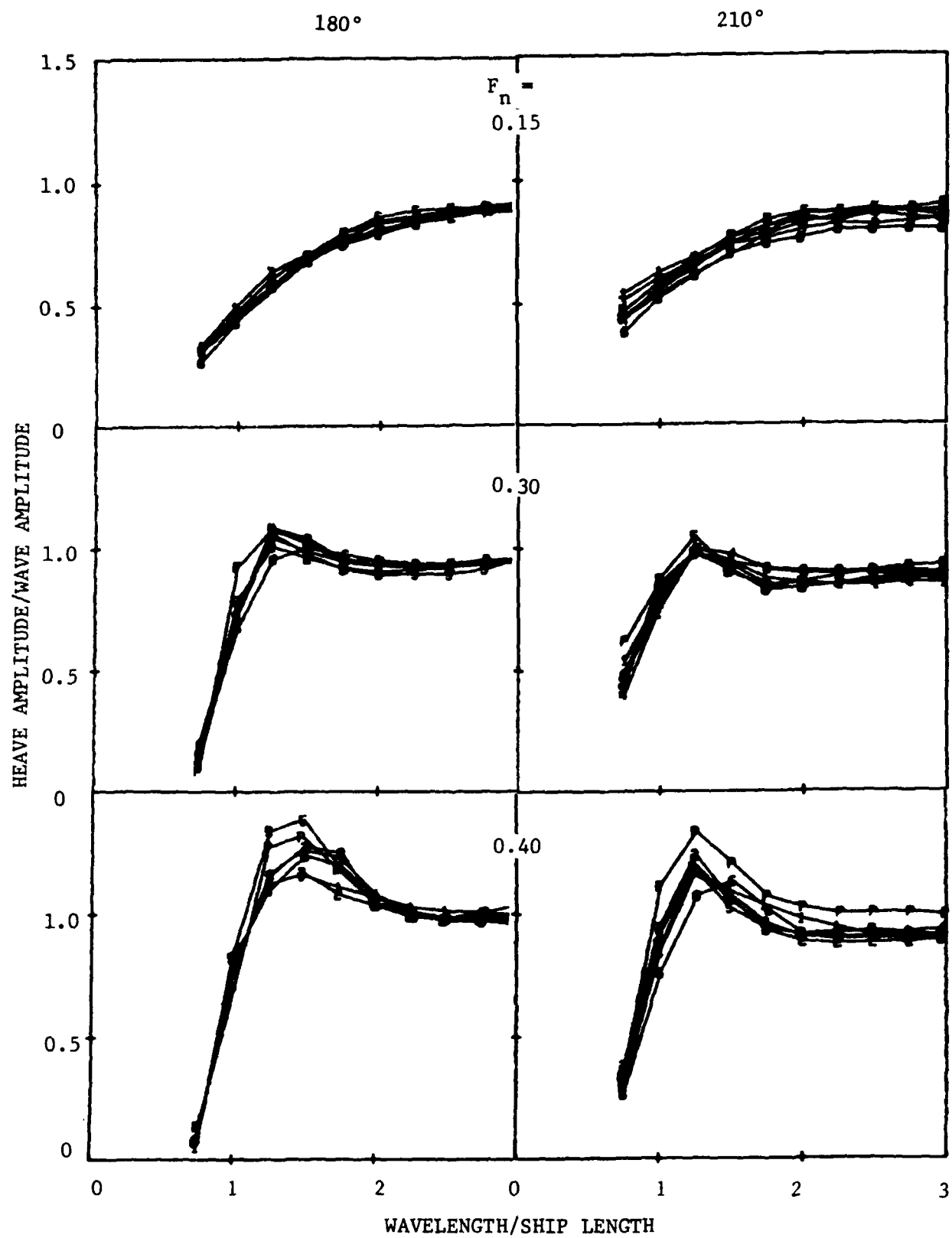


Figure 7 - Nondimensional Heave Transfer Function Comparing the Parent (P) with the Six Bow Variants (1-6)

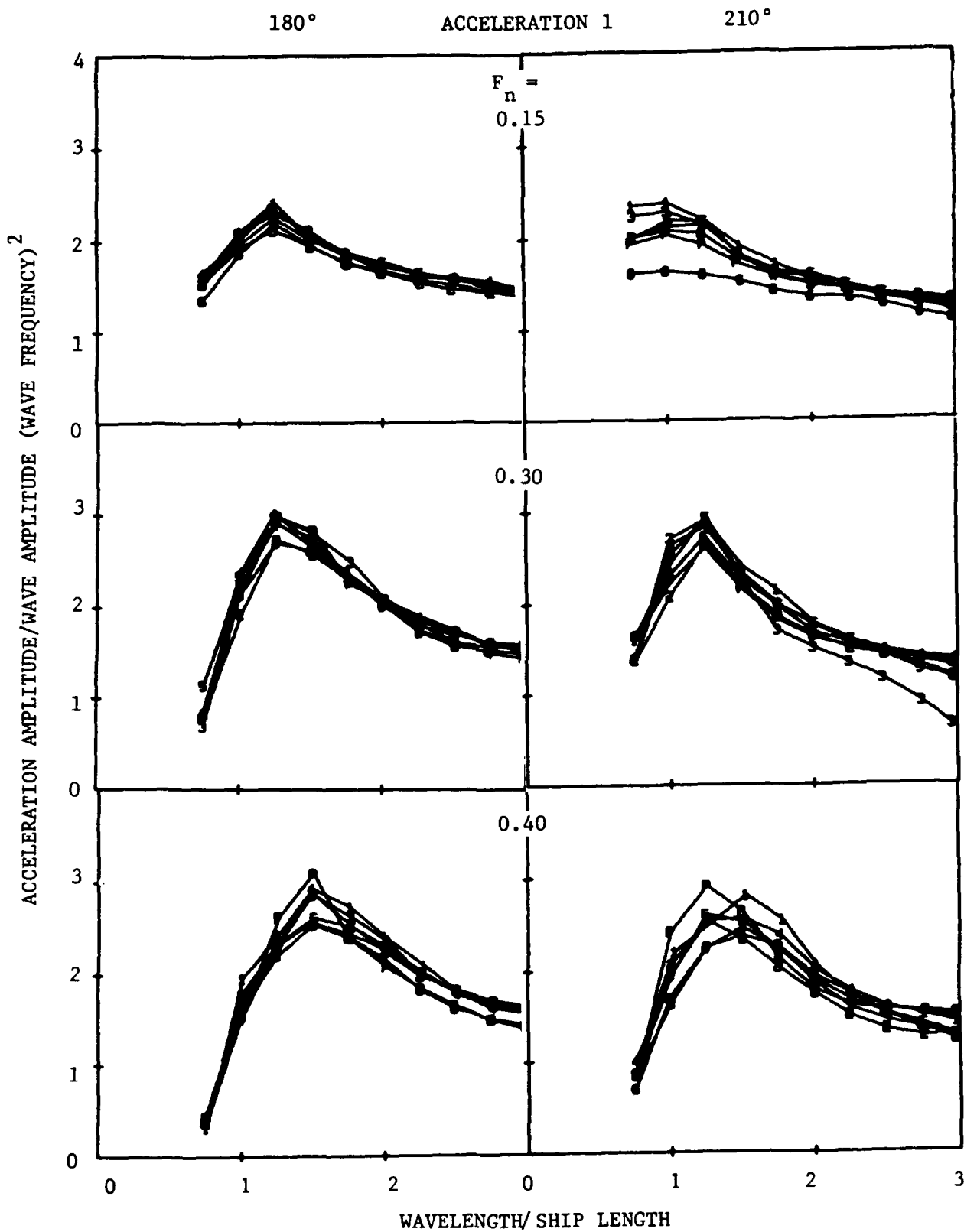


Figure 8 - Nondimensional Acceleration Transfer Function Comparing the Parent (P) with the Six Bow Variants (1-6)

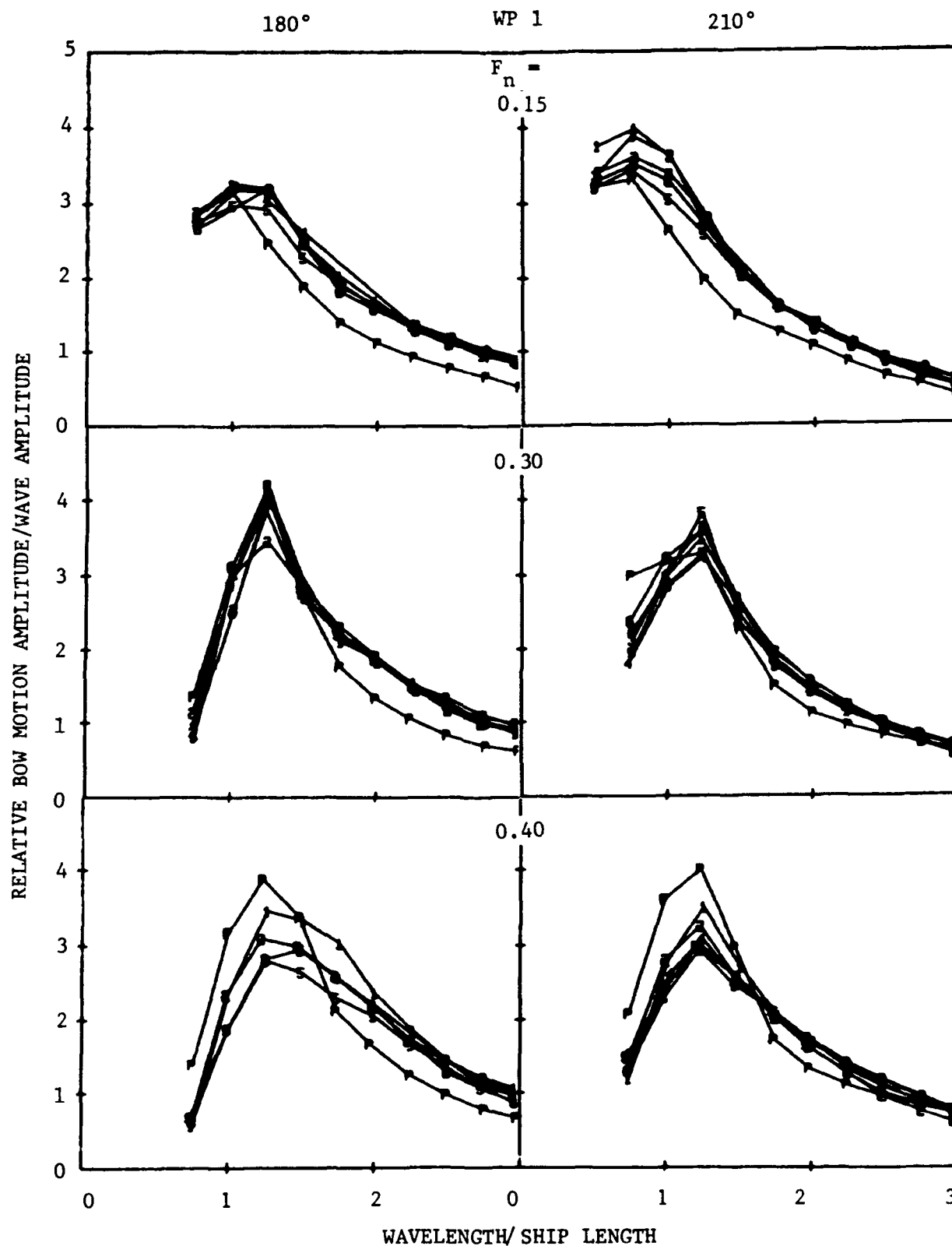


Figure 9 - Nondimensional Relative Bow Motion Transfer Function Forward of the Stem Comparing the Parent (P) with the Six Bow Variants (1-6)

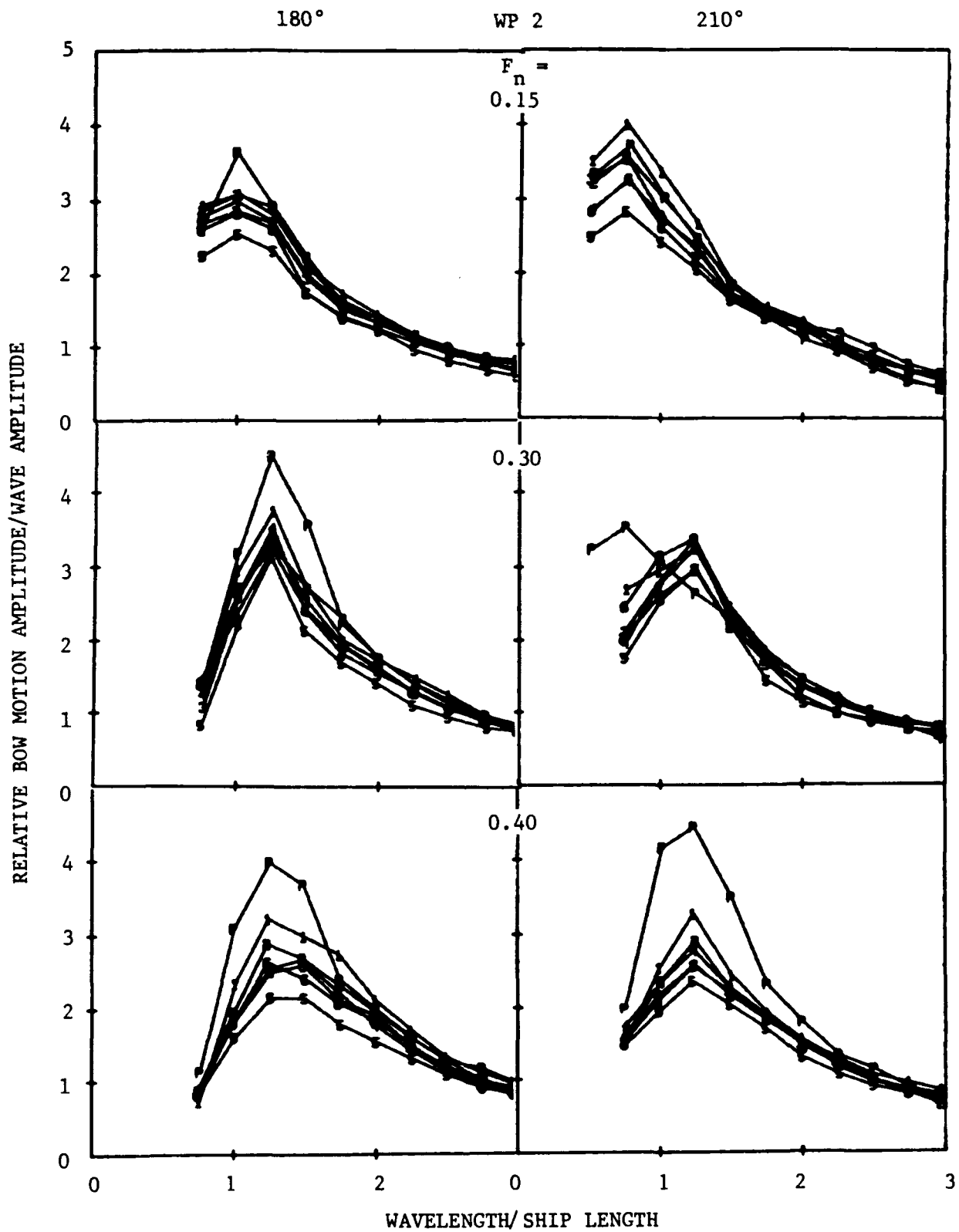


Figure 10 - Nondimensional Relative Bow Motion Transfer Function at Station 0 Port Side Comparing the Parent (P) with the Six Bow Variants (1-6)

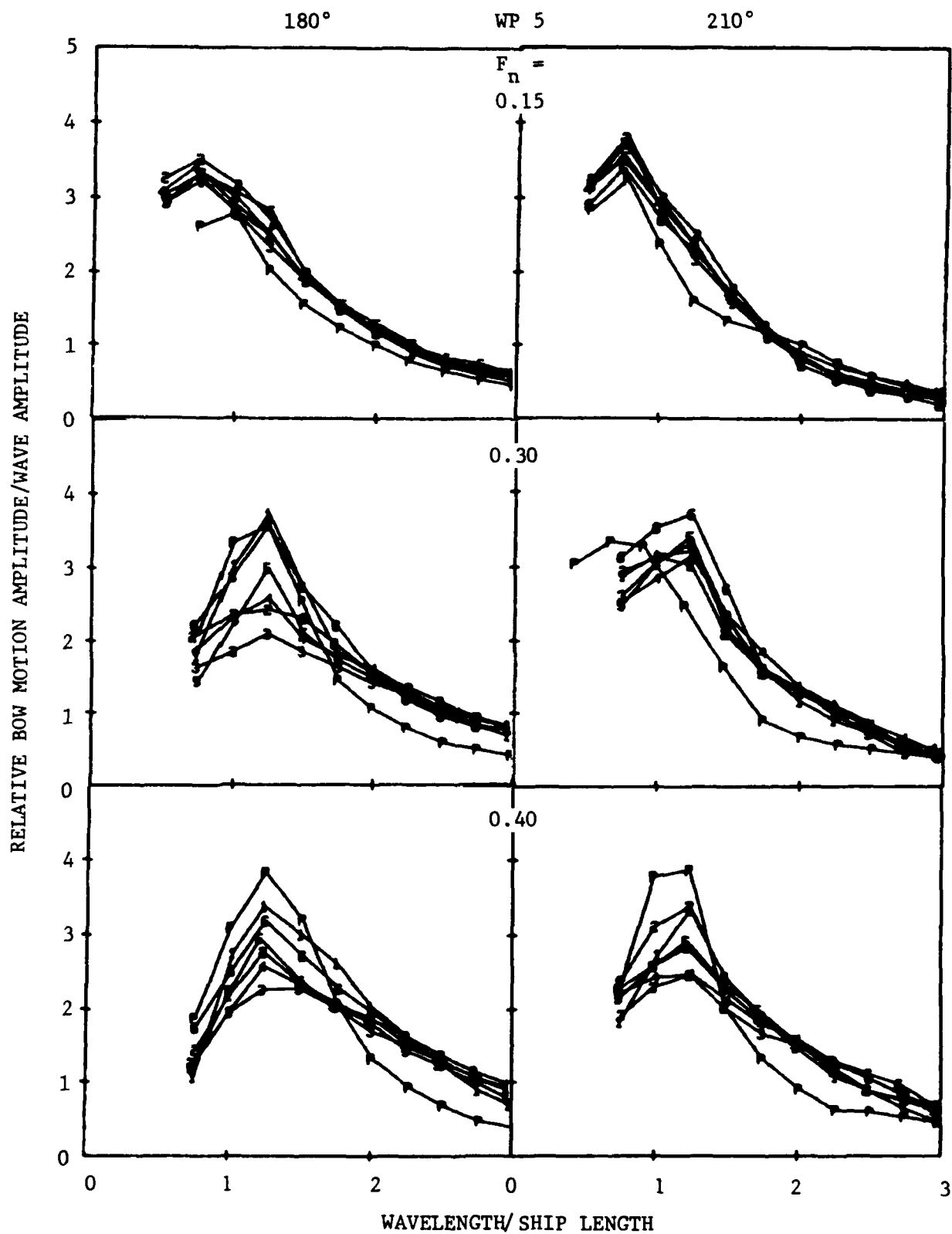


Figure 11 - Nondimensional Relative Bow Motion Transfer Function at Station 1 Starboard Side Comparing the Parent (P) with the Six Bow Variants (1-6)

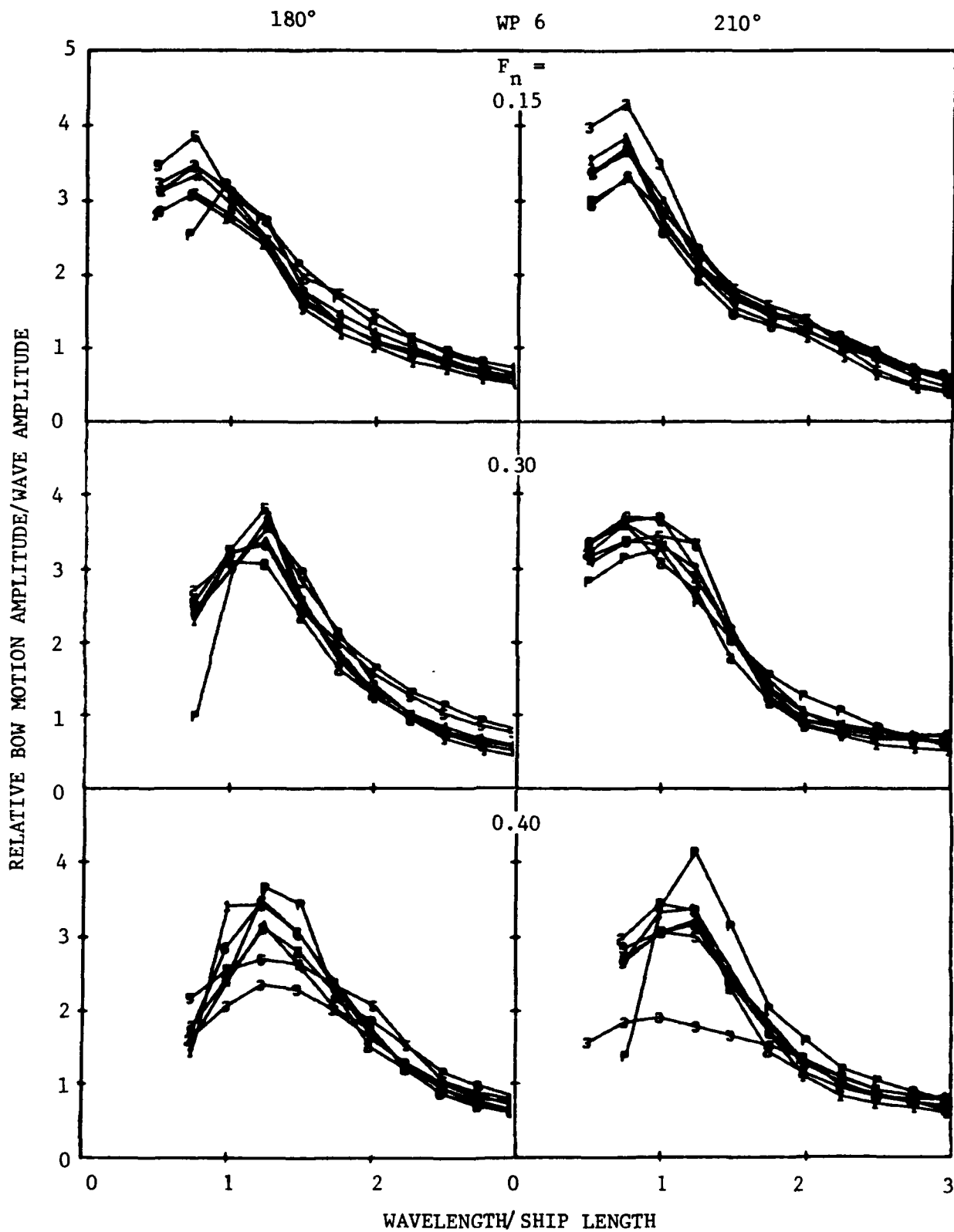


Figure 12 - Nondimensional Relative Bow Motion Transfer Function at Station 2 Port Side Comparing the Parent (P) with the Six Variants (1-6)

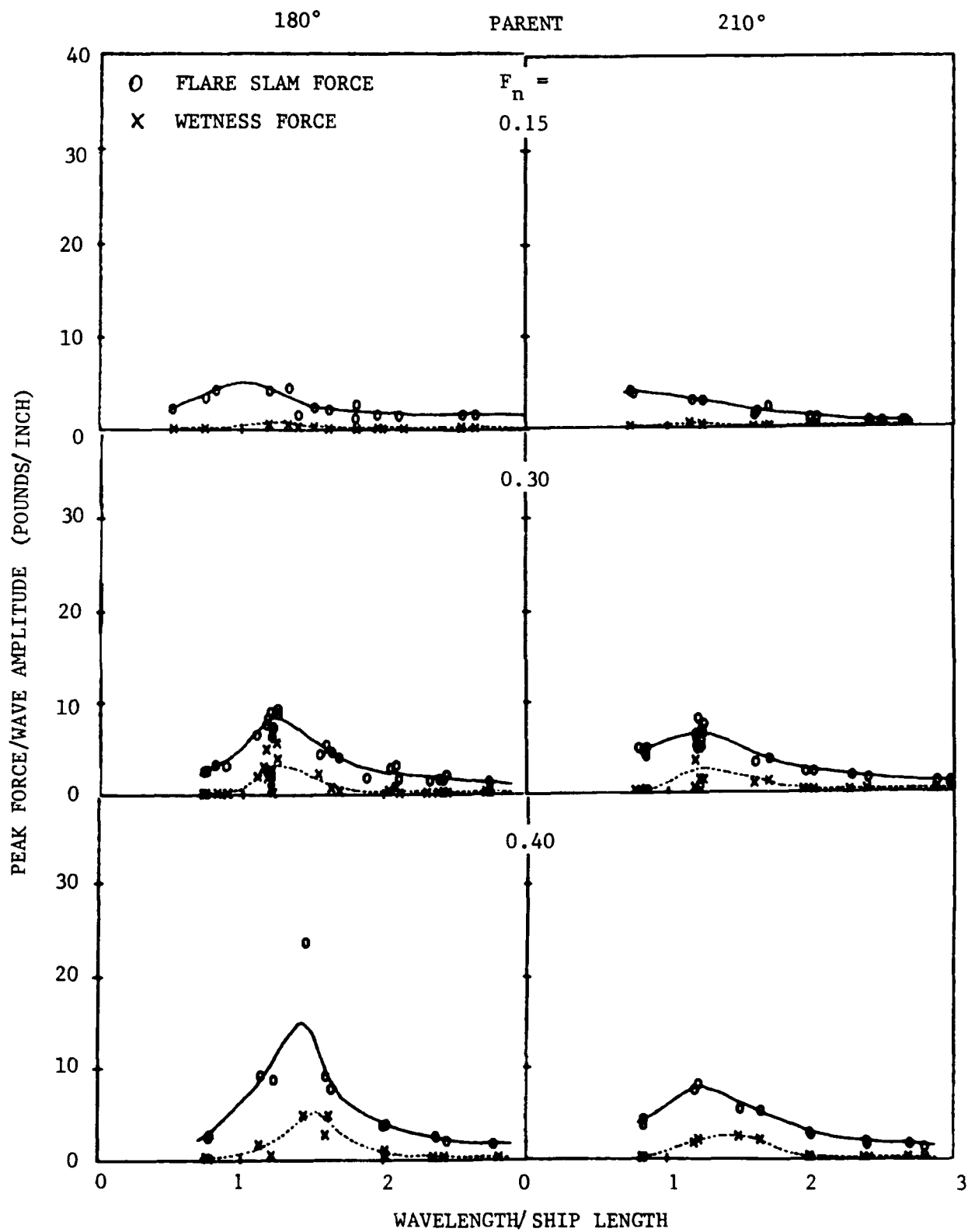


Figure 13 - Peak Flare Slam and Deck Wetness Forces Acting on the Parent Bow Normalized by Wave Amplitude

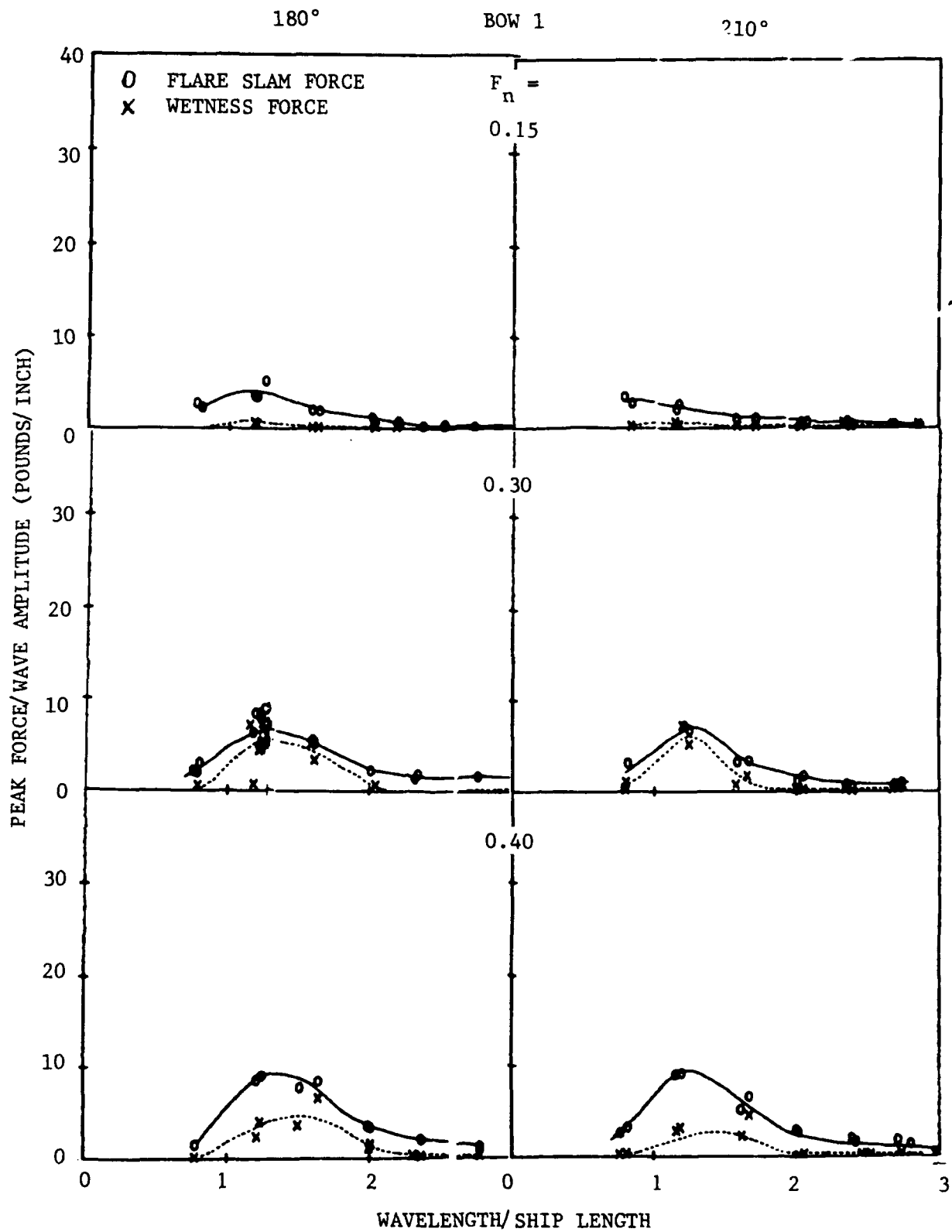


Figure 14 - Peak Flare Slam and Deck Wetness Forces Acting on Bow 1 Normalized by Wave Amplitude

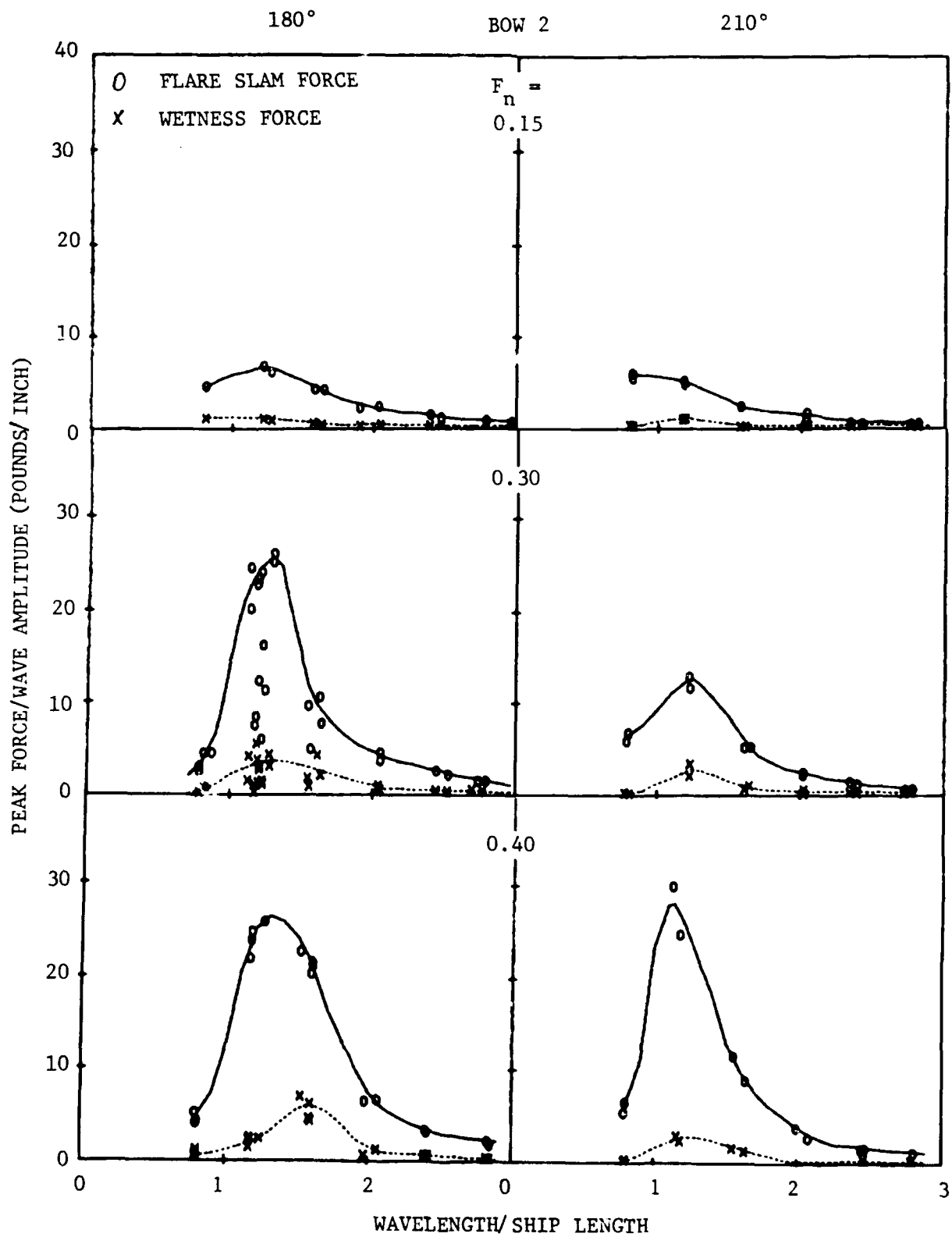


Figure 15 - Peak Flare Slam and Deck Wetness Force Acting on Bow 2 Normalized by Wave Amplitude

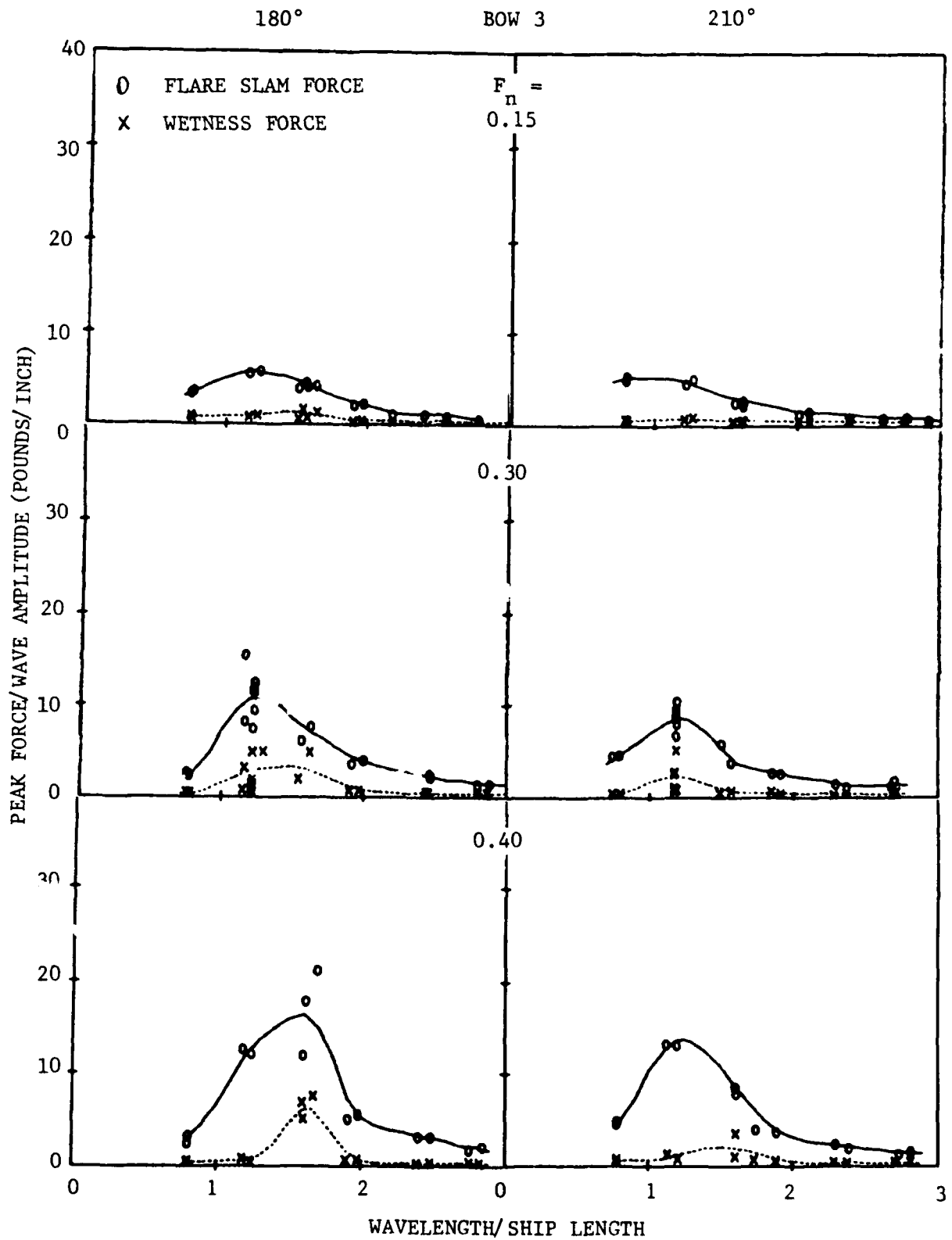


Figure 16 - Peak Flare Slam and Deck Wetness Forces Acting on Bow 3 Normalized by Wave Amplitude

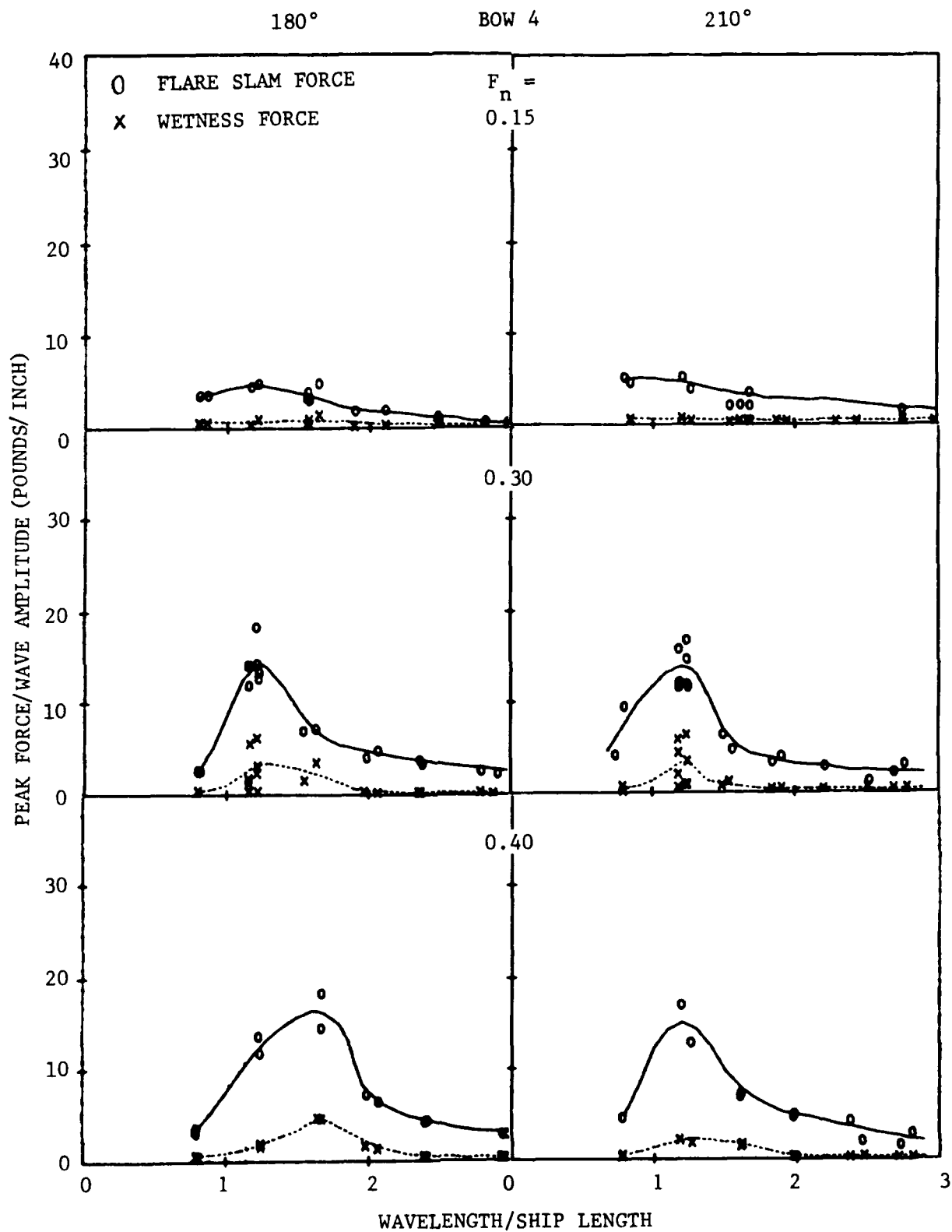


Figure 17 - Peak Flare Slam and Deck Wetness Forces Acting on Bow 4 Normalized by Wave Amplitude

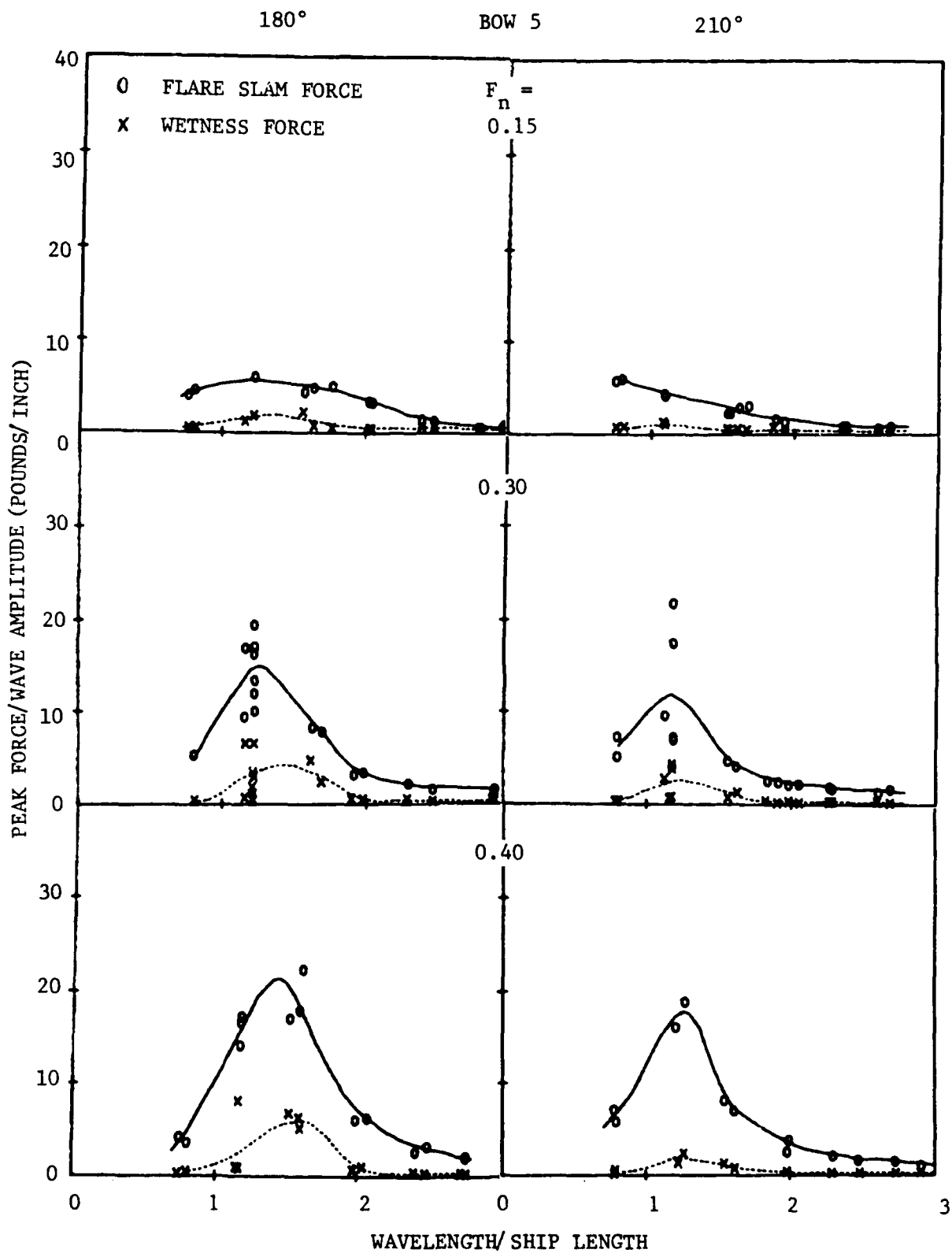


Figure 18 - Peak Flare Slam and Deck Wetness Forces Acting on Bow 5 Normalized by Wave Amplitude

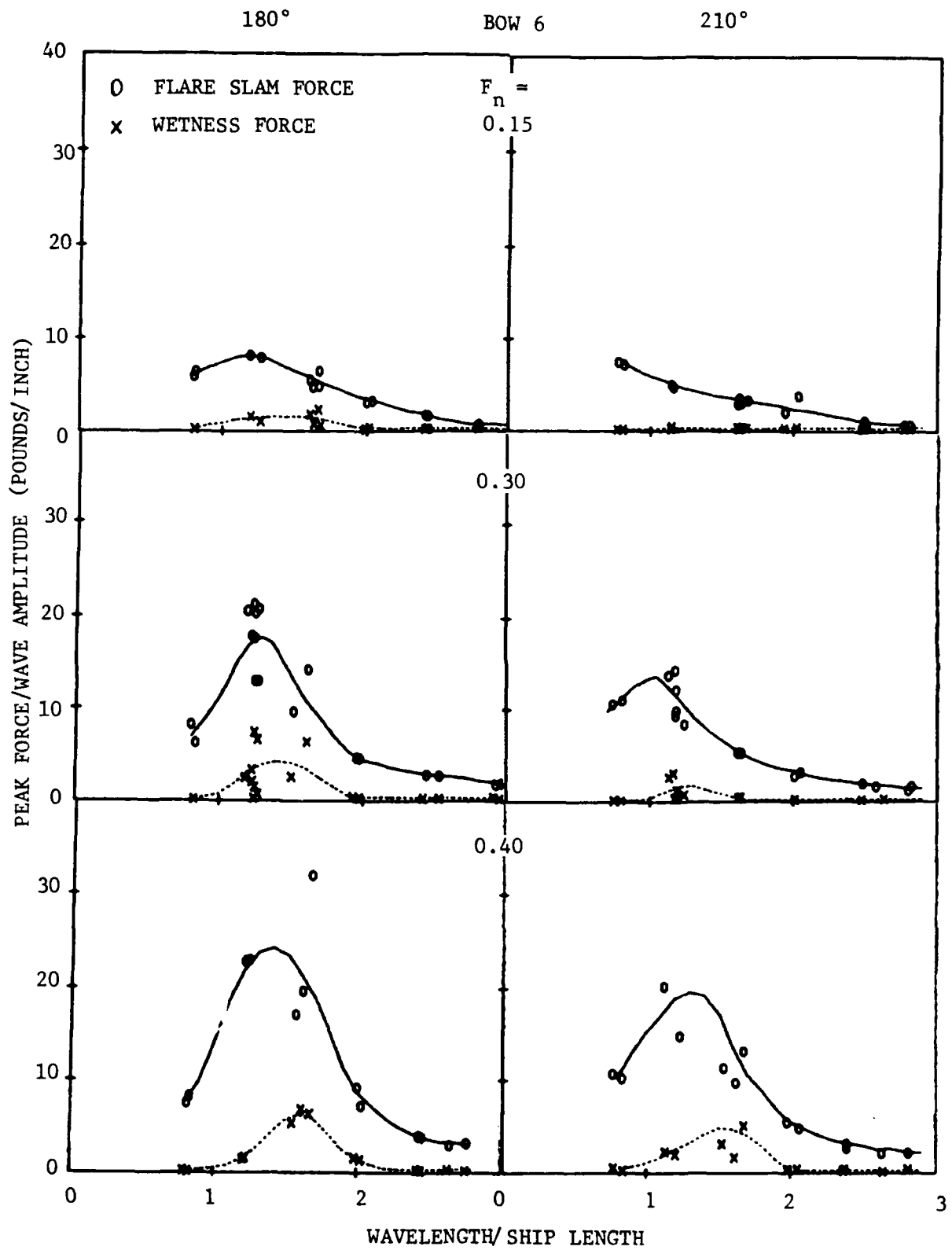


Figure 19 - Peak Flare Slam and Deck Wetness Forces Acting on Bow 6 Normalized by Wave Amplitude

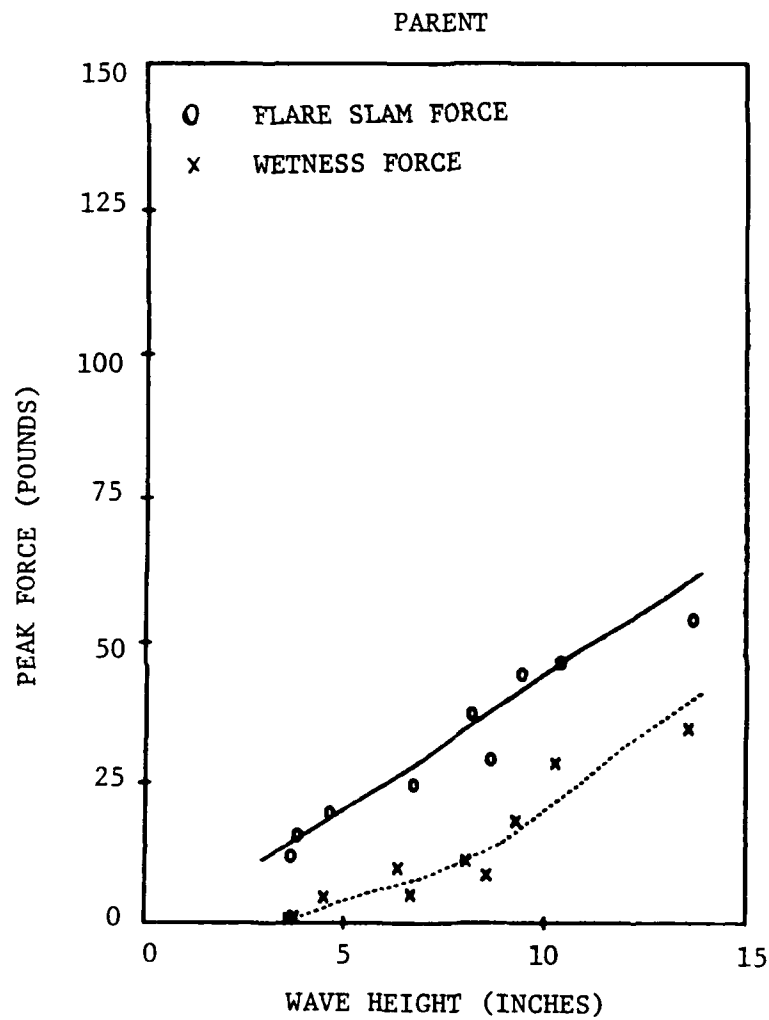


Figure 20 - Peak Flare Slam and Deck Wetness Forces Acting on the Parent Bow versus Wave Height in Head Waves for $\lambda/L = 1.2$ and $F_n = 0.30$

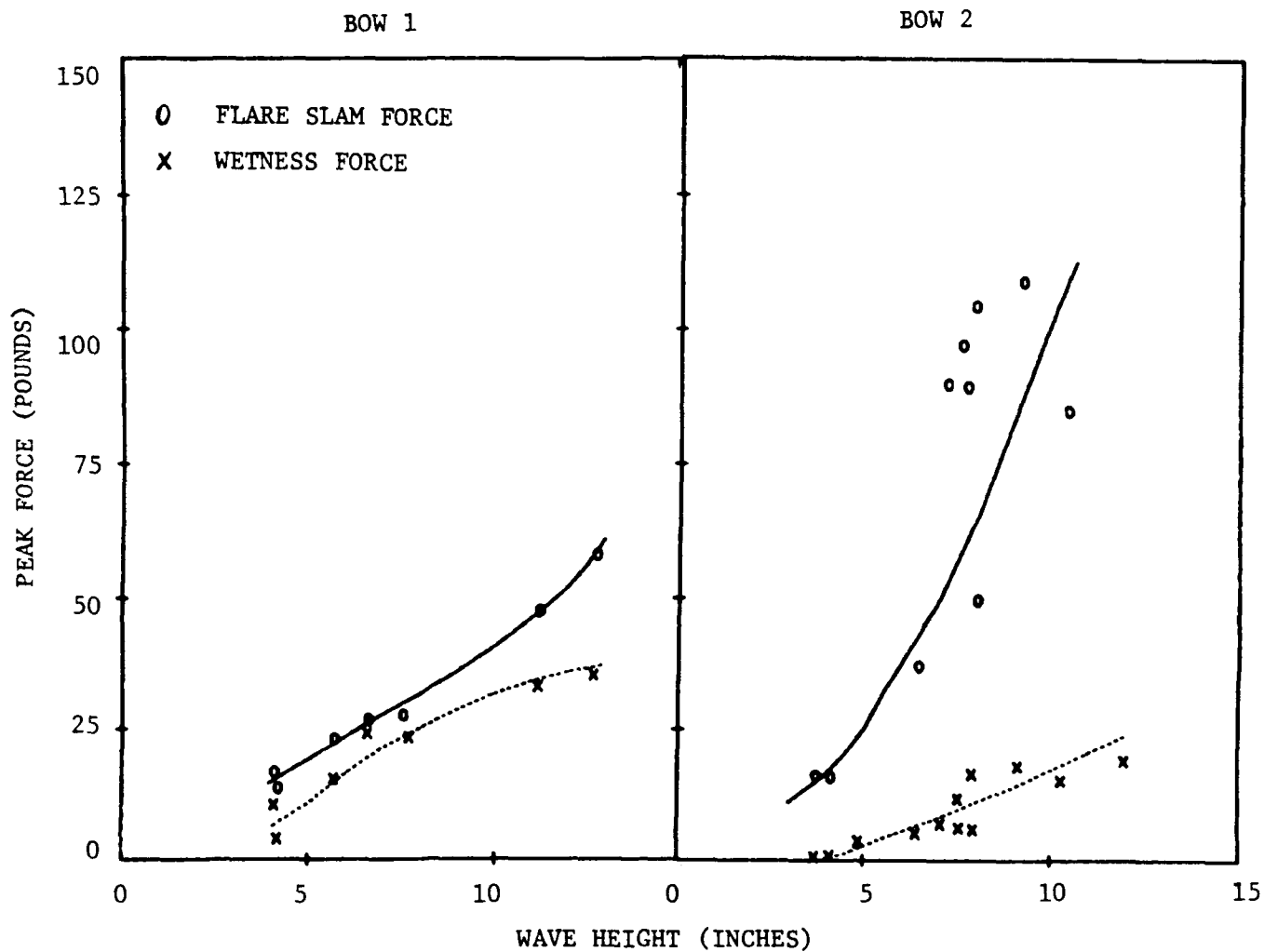


Figure 21 - Peak Flare Slam and Deck Wetness Forces Acting on Bow 1 and Bow 2 versus Wave Height in Head Waves for $\lambda/L = 1.2$ and $F_n = 0.30$

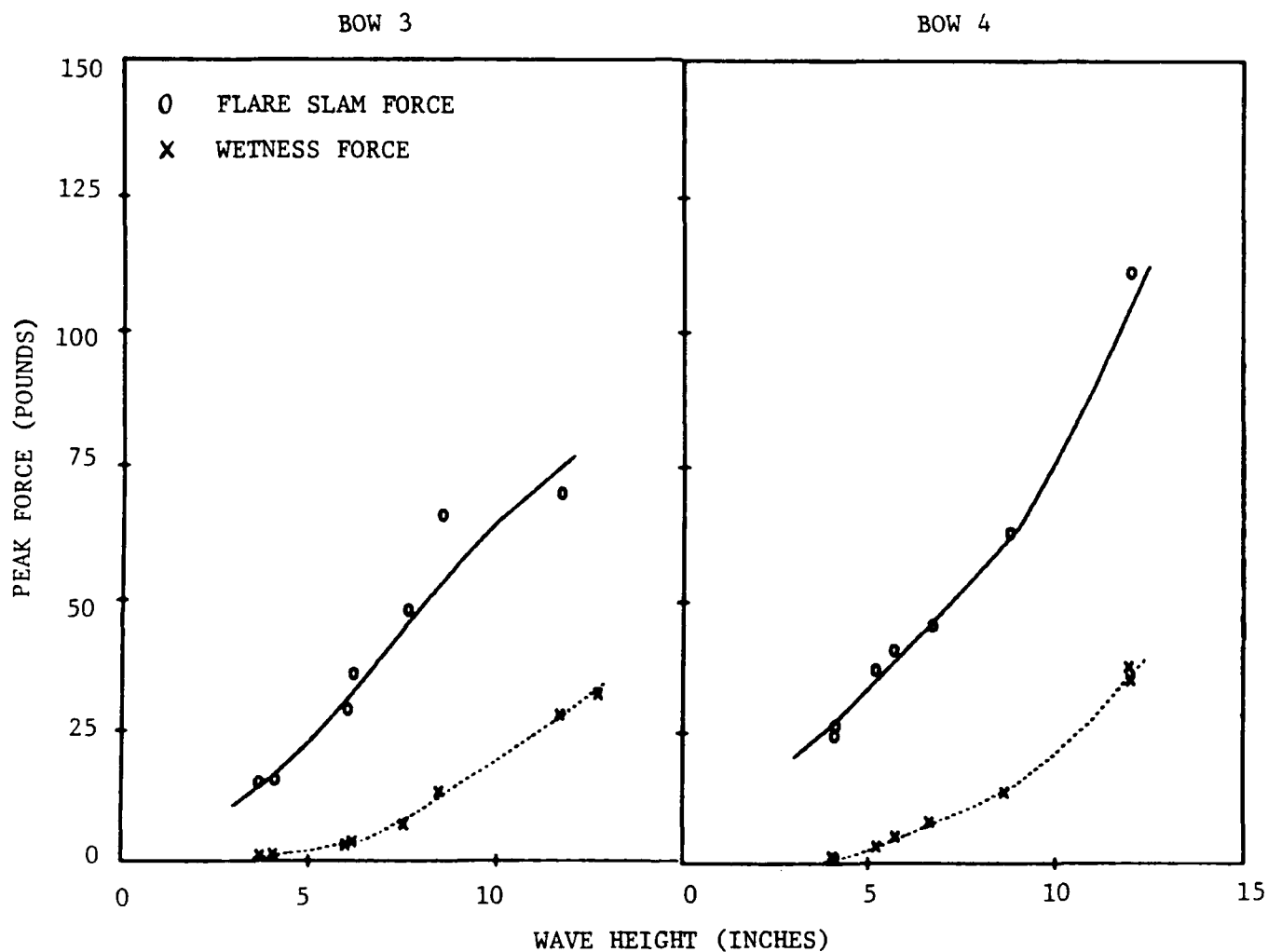


Figure 22 - Peak Flare Slam and Deck Wetness Forces Acting on Bow 3 and Bow 4 versus Wave Height in Head Waves for $\lambda/L = 1.2$ and $F_n = 0.30$

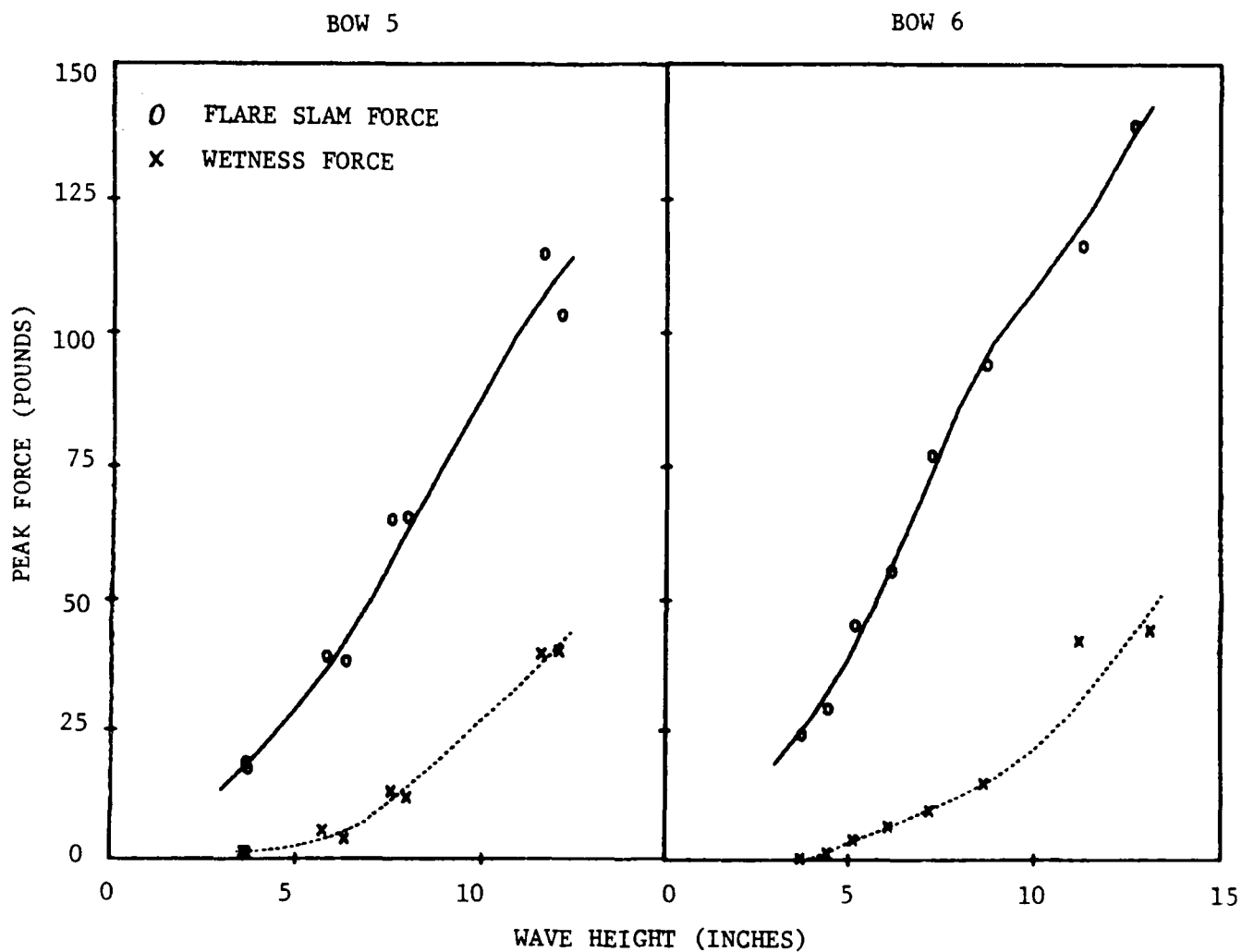


Figure 23 - Peak Flare Slam and Deck Wetness Forces Acting on Bow 5 and Bow 6 versus Wave Height in Head Waves for $\lambda/L = 1.2$ and $F_n = 0.30$

Table 1 - Flare Slamming Model Particulars

Displacement (fresh water) - kilograms,pounds	165	364.4
Length Between Perpendiculars - meters,feet	4.50	14.76
Beam - centimeters,inches	49.6	19.54
Draft - centimeters,inches	16.3	6.427
Tranverse Metacentric Height - centimeters,inches	4.70	1.85
Vertical Center of Gravity above Keel - centimeters,inches	20.3	8.01
Longitudinal Center of Gravity, aft of midships - centimeters,inches	2.50	0.986
Longitudinal Radius of Gyration	0.28Lpp	
Block Coefficient	0.463	
Midship Area Coefficient	0.750	

Bow Variant Particulars

Bow	Model Number	Name	Weight		Area	
			kilograms	pounds	square centimeters	square inches
Parent	5405	Parent	9.2	20.2	1955	303
Bow 1	5405-1	Decreased Flare	7.3	16.2	1370	213
Bow 2	5405-2	Increased Flare	9.0	20.0	2684	416
Bow 3	5405-3	Reflexive Sheer	8.4	18.5	2201	341
Bow 4	5405-4	Reduced Overhang	7.1	15.7	1879	291
Bow 5	5405-5	Shallow Knuckle	8.1	17.9	1955	303
Bow 6	5405-6	Deep Knuckle	8.6	19.0	1955	303

(Left Blank Intentionally)

REFERENCES

1. O'Dea, J.F. and D.A. Walden, "The Effect of Bow Shape and Nonlinearities on the Prediction of Large Amplitude Motions and Deck Wetness," Naval Hydrodynamics presented to the Fifteenth Symposium (1985).
2. Bales, N.K. and H.D. Jones, "Measurement and Reduction of Model-Scale Data on Flare Slamming and Deck Wetness," 19th American Towing Tank Conference (July 1980).